T-3198

SHEAR AND COMPRESSIONAL ANALYSIS OF VSP IN SILO FIELD, DENVER-JULESBURG BASIN

by

T.J. O'Rourke

T-3198

A thesis submitted to the Faculty and the Board of Trustees of the Colorado School of Mines in partial fulfillment of the requirements for the degree of Master of Science (Geophysics).

Golden, Colorado

Date April 4, 1986

Signed: T J O'Rourke

T.J. O'Rourke

Approved: Raymond L. Sengbush

Raymond L. Sengbush

Thesis Advisor

Golden, Colorado

Date 4 April 1986

P R Romig

Phillip R. Romig, Head

Department of Geophysics

ABSTRACT

Compressional and shear VSPs were recorded and processed to determine if valid mode converted shear results can be extracted from a standard compressional VSP using commercially available methods.

The survey area is located in Silo Field, 18 miles northeast of Cheyenne, Wyoming. The field produces from fractured Niobrara limestone. Above is 5000 ft of Pierre shale, the subject of several studies on anisotropy and wave propagation. Below are several potential reservoir sands, including the Codell, D, and J formations.

The VSPs were acquired using Schlumberger's three-axis downhole tool. Sources included two Mertz BSX tandem vibrators (one horizontal and one vertical per truck), one Litton 311 vertical vibrator and two Bolt Omnipulse airgun systems.

Six VSPs were recorded in four passes. The BSX vibrators were positioned 400 ft from the well while the Litton vibrator was at 4500 ft during the first pass. Signals were recorded from each source before moving the tool to the next level, eliminating variations in tool orientation and coupling when comparing the vertical P,

vertical S and offset P surveys. Surveys with the Litton vibrator at 3000 ft offset and the Bolt source at 400 and 1500 ft were each recorded in separate passes.

A waveform sonic was recorded over the interval 6800-8160 ft. No useable signal could be recovered above this point.

Three-component VSP processing adds polarization to the classical single component chain. Wavefields were F-K filtered to remove compressional energy before attempting to extract converted shear reflections from the compressional data.

Shear results can be extracted from compressional VSP surveys, using commercially available methods. Results of the same mode (P, SV, SH) generally show a good match of events and character. Comparison of events between modes is fairly consistent, but character matches are often poor.

Amplitude differences may be due to different responses to the same horizon by different modes. Without information from a shear source, quantitative applications of converted results must be treated as indications only, until these differences can be explained.

TABLE OF CONTENTS

TABLE OF CONTENTS (continued)

LIST OF FIGURES

LIST OF FIGURES (continued)

LIST OF FIGURES (continued)

LIST OF TABLES

ACKNOWLEDGEMENTS

With sincere appreciation, I acknowledge the following people who have contributed so much to this work.

I am deeply grateful for the guidance and assistance of my graduate committee, Dr. James E. White and Dr. Frank A. Hadsell, and especially for my advisor, Ray Sengbush, who, in addition to his patience and availability, offered many pertinent observations at critical points in this work.

My thanks go to the consortium of sponsors who provided the funding for acquisition of the VSP data. The sponsors are:

Bolt Technology	CGG American Services, Inc.
Conoco, Inc.	Champlin Petroleum Company
Enserch Exploration, Inc.	CSM Center for Potential Fields
Exxon Production Research	Diamond Shamrock Corporation
Geosource	Mobil Research and Development
Intevep, S.A.	Schlumberger Well Services
Sohio Petroleum Company	Union Oil Co. of California

My thanks also go to Amoco Production Company for allowing us access to the well.

Special thanks to two Schlumberger divisions, Schlumberger Overseas for allowing me the time and providing financial support to pursue this study and Schlumberger Well Services for providing the facilities and computer time to process the data.

I wish to thank Jeff Bond, John Gross, Phillip Lagasse and Dr. Ulrich Schimschal, all with SWS-Denver, for their assistance, technical advice and, most importantly, time at various stages of this project.

Without the help of Marshall Martin and Dr. Tom Davis, this project may never have occurred. Their fracture detection project attracted most of the consortium sponsors and provided the organizational framework to which the VSP study was appended.

Most importantly, I owe my wife, June, a debt I may never be able to repay, for the support, love and understanding she has provided ever since we married, long before this project started. I am also grateful for the support of my children, Andrea and Craig.

INTRODUCTION

With the advent of three component VSP recording capability, classical approaches to acquisition and processing must be reconsidered.

Processing objectives have traditionally been to isolate the pure compressional reflection, removing all else as undesired noise. Often coherent, this "noise" may be converted shear wave modes.

If these modes could be enhanced and extracted, a more detailed analysis could be performed on data without appreciably increasing acquisition costs.

Potential applications include fracture identification, lithology and porosity determination and confirmation of direct hydrocarbon indicators observed on compressional data.

Such applications require accurate compressional and shear velocities, polarizations and amplitudes. Studies of propagation effects such as attenuation and anisotropy may yield additional information.

Implementation of these applications requires greater attention to detail in processing, acquisition techniques and equipment design.

Compressional and shear VSPs were recorded and processed to determine if valid mode converted shear results can be extracted from a standard compressional VSP using commercially available methods.

The survey area is located in Silo field, 18 miles northeast of Cheyenne, Wyoming (fig 1). The field produces from fractured Niobrara limestone. Above is 5000 feet of Pierre shale, the subject of several studies on anisotropy and wave propagation. Below are several potential reservoir sands, including the Codell, D and J formations.

This site was chosen to complement surface shear and compressional seismic surveys acquired for a fracture determination study. The tie between preliminary compressional seismic results and the compressional VSP and synthetic is presented in figure 2. The top of the Niobrara is at 1.77 sec. Codell, D, and J sands are among events between 1.9 and 2.1 sec and the top of the Pierre shale is just above 0.8 sec.

No automatic gain control has been applied to any VSP display in this thesis. The plotting routine normalizes on a trace by trace basis, thus amplitude comparisons are not straightforward.

Two reflected shear wavefields are present in the compressional data. Converted P-SV reflections are generated as the direct P arrival passes through an

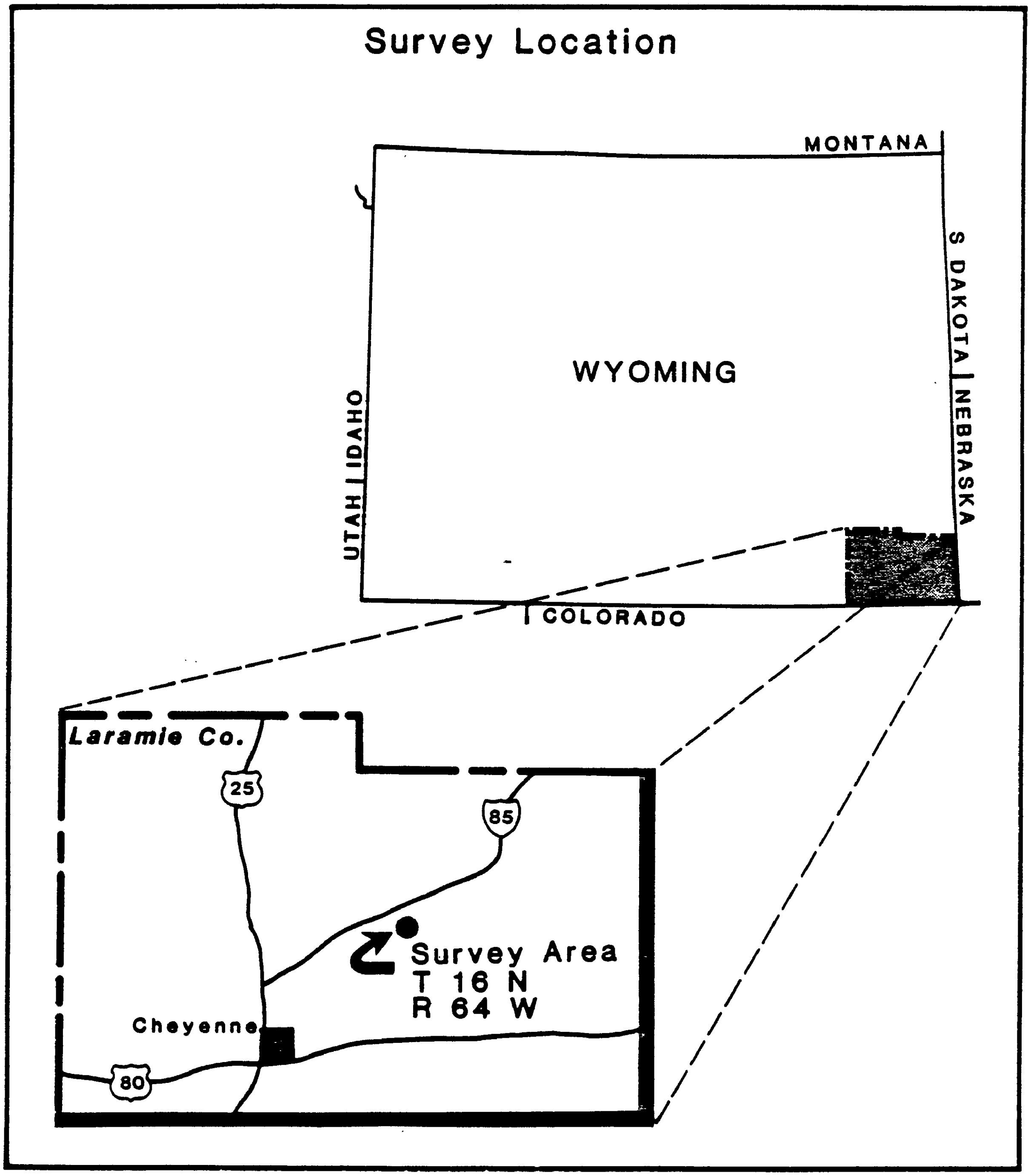

Figure 1. The survey area is located in Silo Field, 18 miles northeast of Cheyenne, Wyoming.

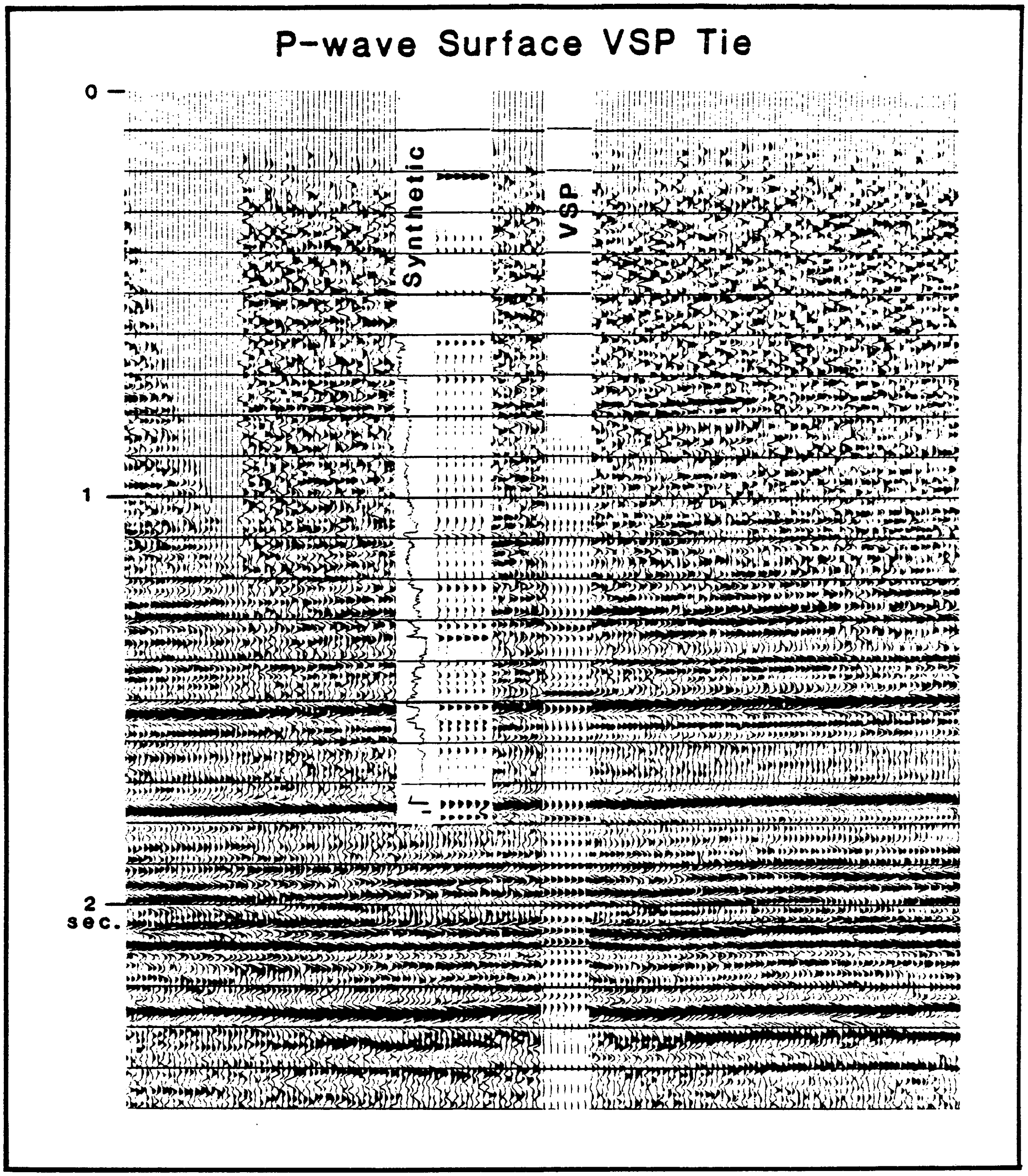

Figure 2. Tie between compressional results of seismic, VSP and synthetic. Top of Niobrara is at 1.77 sec.

interface. A second set of shear reflections occurs when a strong shear arrival, generated at surface, passes through these same horizons. The latter will be referred to as P-S-S reflections for convenience.

ACQUISITION

Six VSPs and a waveform sonic survey were recorded in the well State of Wyoming Y-2, located 4800 ft west of the surface seismic line in sec. 32 of 16N 64W (fig. 3). This vertical well was drilled by Amoco Production Company in May 1984. Table I recaps well conditions at the time of acquisition, November 10-13 1985. Pumps in nearby producing wells generated 15 Hz noise during acquisition.

Equipment

The VSPs were acquired using Schlumberger's three axis SAT[R] downhole tool and CSU[R] surface recording system. The hydraulically anchored SAT tool uses one 10 Hz geophone per axis, transmitting data to surface in digital form, at 2 ms sample rate. Lower frequency geophones would be preferred for shear measurements, but are more sensitive to rough field handling and pose greater difficulties in matching horizontal and vertical responses.

Sources included two Mertz BSX vibrators, one Litton 311 vibrator and two Bolt Omnipulse airgun systems. The BSX is a tandem vibrator, having dual electronics and vibrating units. These were configured with one vertical

[R] Schlumberger trademark

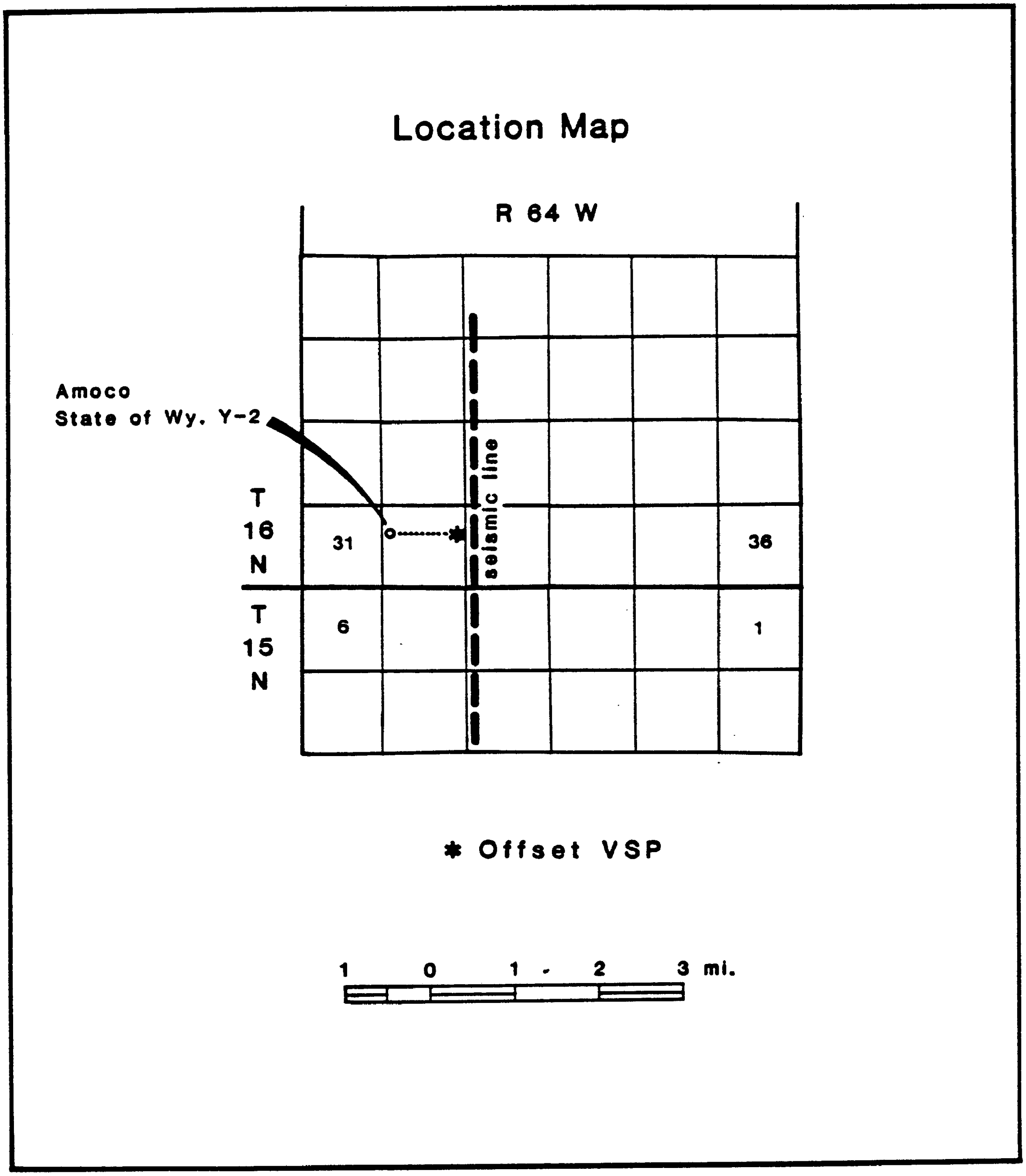

Figure 3. Location map for VSP and seismic line. The well is 4800 ft west of the seismic line.

TABLE I

WELL CONDITIONS

original TD	8258		
survey TD	8165 - debris below		
Open Hole	7925 - 8165		
Bit Size	6 1/8"		
Casing	7"	0 - 7925	
	9 5/8"	0 - 1981	
Fluid	crude oil - top at 2800		
	open hole interval drilled with crude		
		Run	Interval
Logs available	sonic	1	1980 - 7876
		2	7916 - 8258
	density	1	7916 - 8258

and one horizontal unit on each truck, increasing the holddown weight available in either mode. The Litton 311 is a single vertical vibrator. Consistent freezing temperatures during the acquisition greatly improved source coupling.

Procedure

Acquisition parameters are listed in Table II while figure 4 illustrates source positions and survey intervals. Note the east-west line along which the sources were positioned is 180 ft south of the well. Offsets reported are direct well-to-source distances. Preliminary modeling indicated the reflected P-S conversions should be maximized in the region of the 4500 ft offset.

The six VSPs were recorded in four passes. The BSX vibrators were positioned 400 ft from the well while the Litton vibrator was at 4500 ft during the first pass. Signals were recorded from each source before moving the tool to the next level, eliminating variations in tool orientation and coupling when comparing the vertical P, vertical S and long offset P surveys.

The 3000 ft vibrator offset and Bolt 400 and 1500 ft offsets were each recorded in separate passes. The surveys using the Bolt Omnipulse were run as a source

TABLE II

ACQUISITION PARAMETERS

PARAMETER	P SURVEYS	SH SURVEYS
Vibrator	2xBSX + Litton 311	2 x BSX
Sample Rate	2 ms	2 ms
Sweep frequency	8 - 96 Hz	4 - 52 Hz
Sweep length	8 sec.	8 sec.
Min. sweeps	3	3

SURVEY	SOURCE	OFFSET	INTERVAL	LEVELS
1	P BSX	400	500-8160	87
2	SH BSX	400	500-8160	87
3	Litton	4500	4000-8160	73
4	Litton	3000	5950-7000	15
5	Bolt	400	5950-7000	15
6	Bolt	1500	5950-7000	15

Level spacing	surveys 1,2,3	surveys 4,5,6
50 ft	6050-8160	
75	4100-5975	5950-7000
100	3000-4000	
500	500-2500	

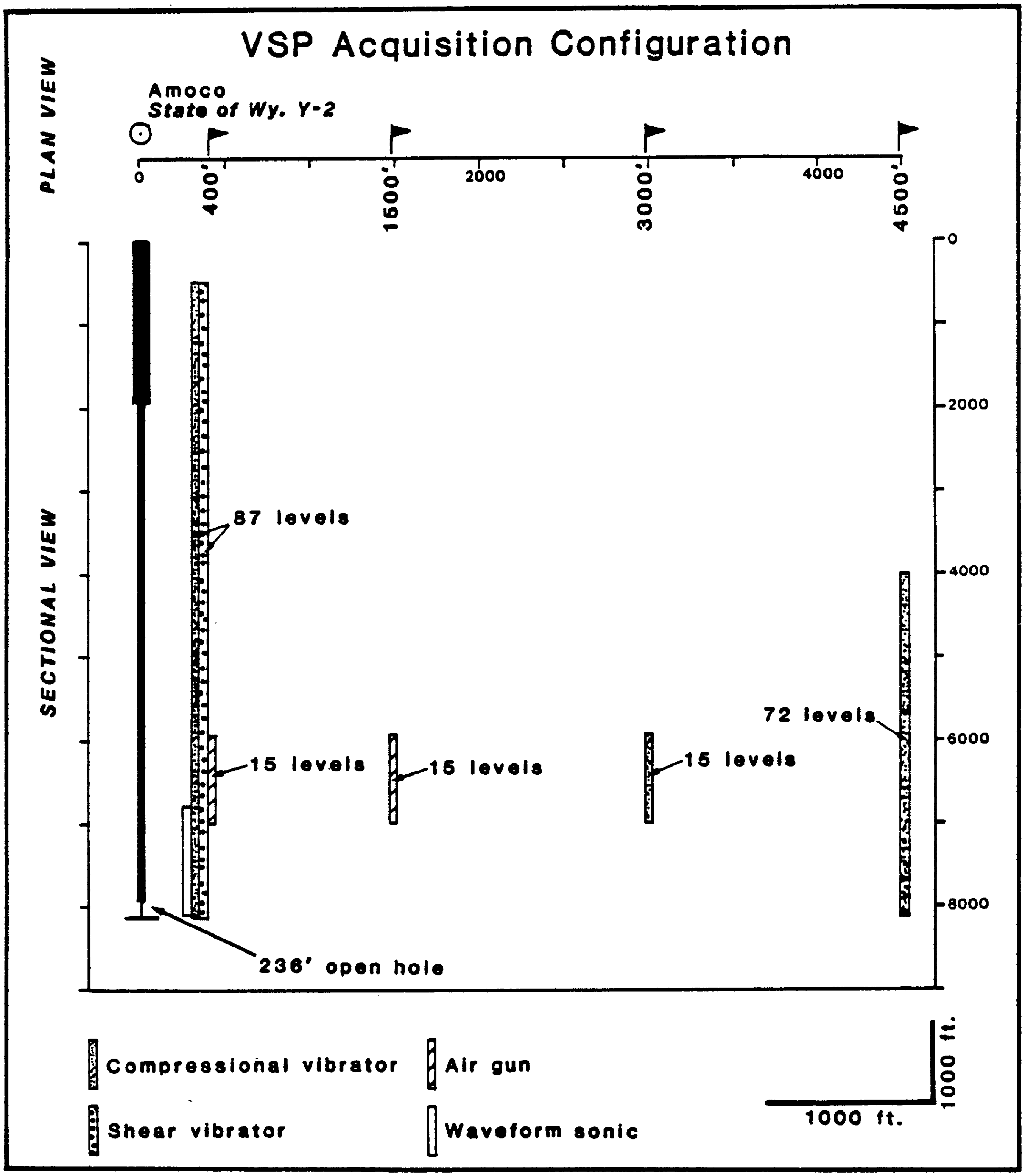

Figure 4. Six VSPs acquired in four passes. To ensure similar tool response, the surveys of 87 and 72 levels were taken in one pass.

comparison test and are reviewed in Appendix A. The 3000 ft vibrator survey fills in offset positions for potential future studies.

VELOCITY LOGS

The waveform sonic was recorded over the interval 8160 to 6800 ft. No useable signal could be recorded above this point, probably due to lack of bonding between formation and casing. Open hole logs, recorded at the time of drilling, were patched to extend the sonic to within 2000 ft of surface. The shear velocity determined from the waveform sonic has been extended with interval velocities from the shear VSP, which are not as accurate.

Logs in figure 5 have been corrected for drift. Drift is the difference between VSP arrival times and times from integration of the sonic log. Seismic times are assumed to be correct and sonic values may differ because of noise, borehole and frequency effects. Though the shear log is coarse, the curves are similar and have been used for subsequent modeling.

A low-velocity shear zone between 3200 and 3600 ft is evident on the velocity ratio curves of figure 6. Both average and interval curves are ratios from P and SH input data. The pronounced velocity ratio anomaly can not be explained with information currently available. Anisotropic effects are postulated. (see Appendix C).

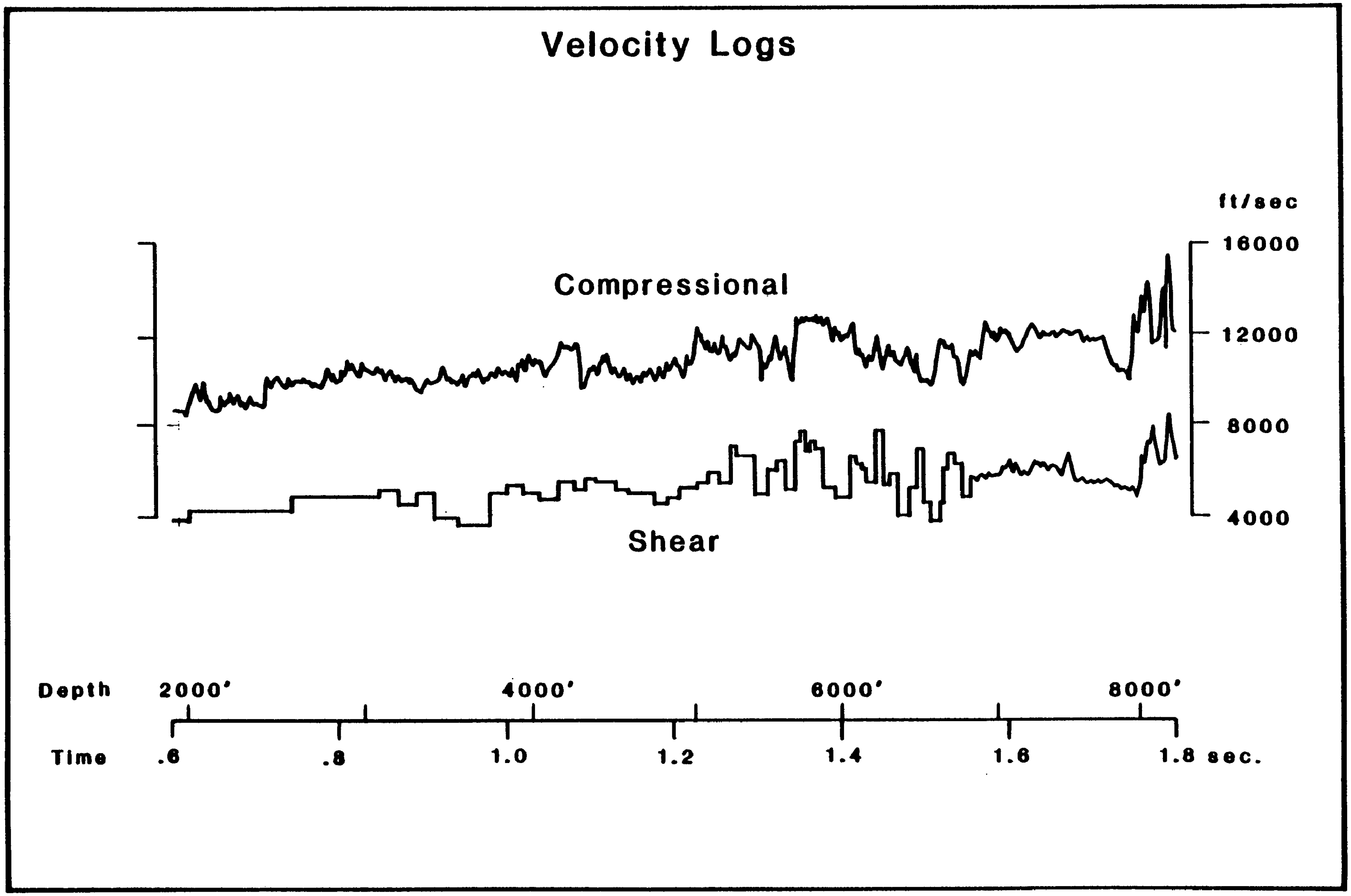

Figure 5. Compressional and shear velocity logs. Shear velocities above 6800 ft are from VSP interval velocities.

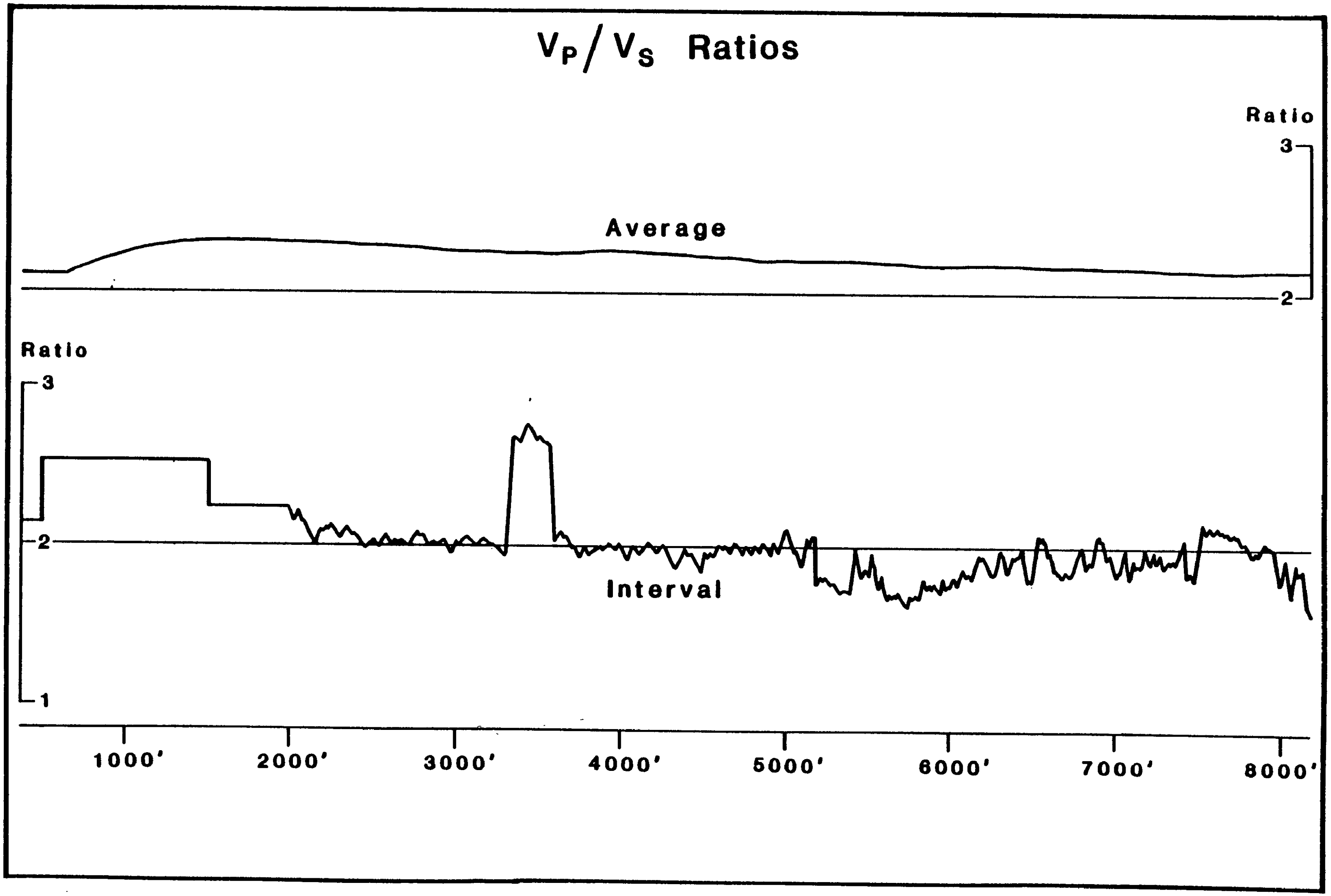

Figure 6. Average and interval velocity ratios. The anomaly between 3200 and 3600 ft is believed to be due to anisotropy, as discussed in Appendix C.

POLARIZATION

Polarization prepares three component data for classical single component processing. The procedure compensates for tool rotation and tends to enhance different types of waves for subsequent processing.

Polarization Theory

Polarization is performed in two stages, as illustrated in figure 7. Hodograms, polarization angles and correlation measures of ellipticity are used to monitor the quality of the process. Hodograms (fig 8) display the velocity trajectory by plotting X(t) versus Y(t) in a small time window surrounding the first arrival.

Because records are contaminated by noise, the curve should be an ellipse rather than a straight line (assuming plane waves in a homogeneous medium). The major axis defines the main direction of energy arrival in the horizontal plane. For a compressional signal, this points towards the source, establishing a fixed reference axis, consistent from level to level, irrespective of tool rotation.

Once this axis is determined, a coordinate transformation from (X,Y) to (Hmax,Hmin) is performed. The

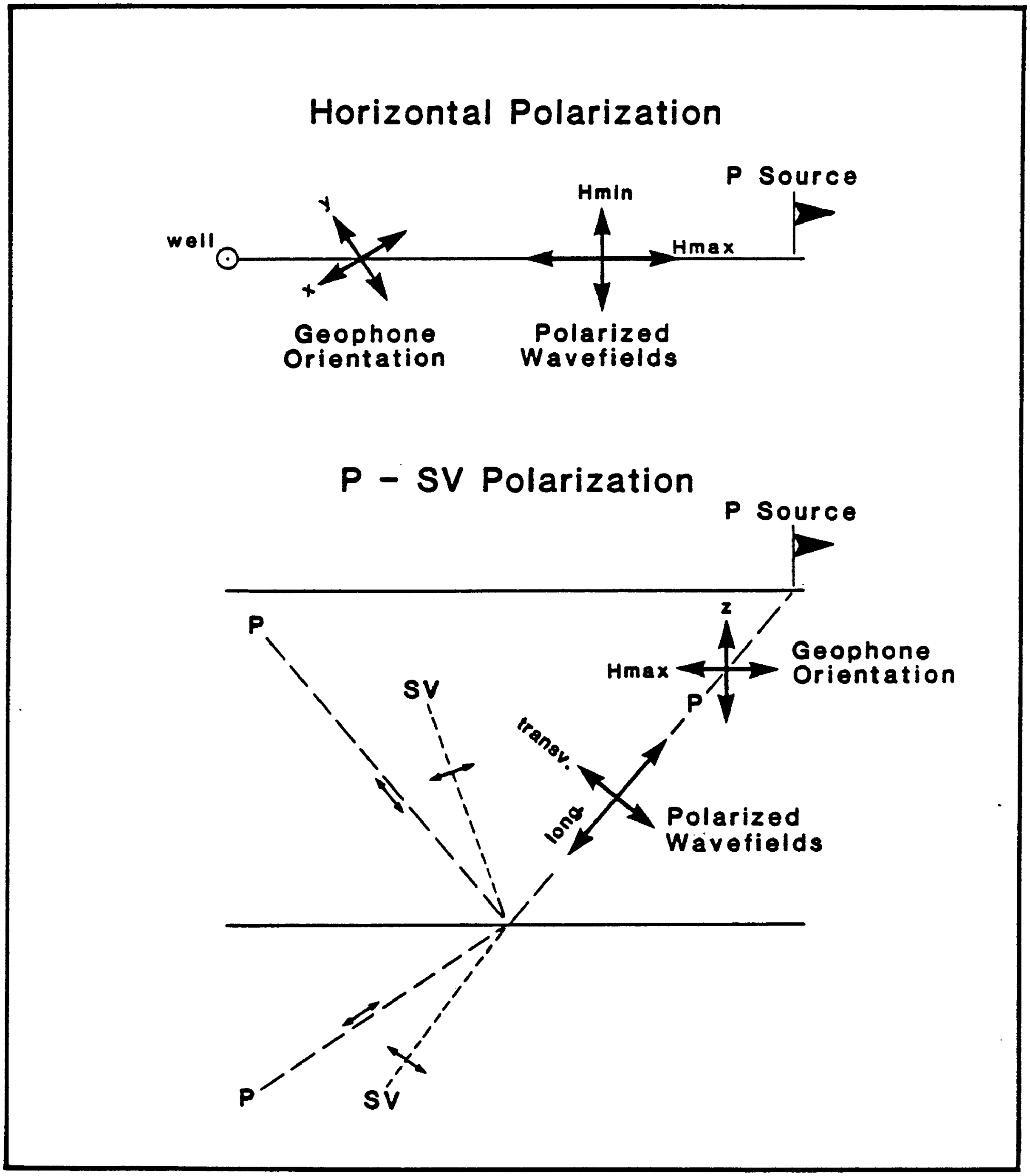

Figure 7. Polarization is performed in two stages. Longitudinal and transverse orientations enhance in-plane motion of P- and SV-waves.

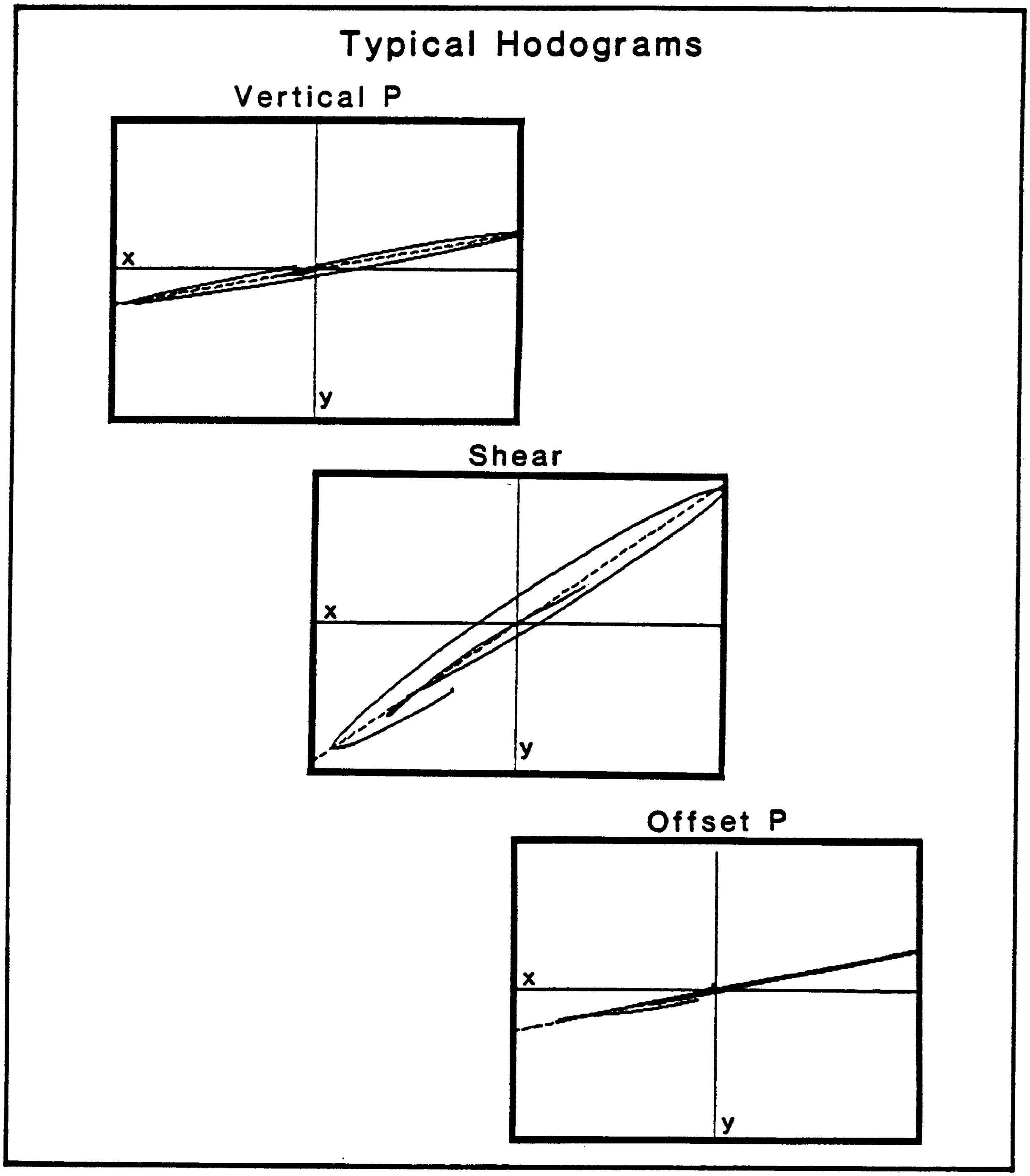

Figure 8. Hodograms display velocity trajectory by plotting X(t) vs Y(t) in a small window around the first arrival.

Hmax axis is in the direction of maximum particle velocity with the Hmin axis perpendicular to this (not a true minimum if the ellipse is skew).

Assuming linear polarization, the Hmax axis represents the in-plane motion of P and SV waves, while Hmin should enhance the SH wavefield. If we had a pure P-SV source, a true visco-elastic medium and perfect horizontal layering, we should observe only noise in the Hmin axis.

Components of the in-plane P-SV wavefield can be further enhanced by polarizing the Z and Hmax axes into longitudinal and transverse axes. These final axes represent particle velocity in line with and normal to the ray of the direct P arrival, respectively.

As illustrated in figure 7, the longitudinal wavefield tends to enhance direct P and reflected SV energy for offset sources. The transverse wavefield then enhances reflected P and direct SV energy. For small offset configurations, the longitudinal axis represents the P wavefield while the transverse axis contains the total SV energy.

Polarization Results

The polarization procedures appear to have performed well. The mixed energies in both the longitudinal and transverse data files can be easily separated with velocity or F-K filters during subsequent processing.

A strong direct P arrival followed later by a ringing SV event is evident on the Hmax wavefield from the 400 ft offset compressional vibrator (fig 9). This event can not be a tube wave, for reasons discussed in Appendix C. The precursors to the downgoing SV are P-S conversions, occurring near surface. Converted shear reflections can be seen originating from the direct P arrival at 0.89 sec and below TD at 1.17 sec.

Both Hmax and Hmin (fig 10) contain a surprising amount of coherent shear energy for this acquisition geometry. The Hmax wavefield contains greater energy than the Hmin where more random events of larger amplitude indicate a poor signal-to-noise ratio. Normalization in the plotting routine has amplified the Hmin display. The indistinct direct P arrival indicates the out-of-plane nature of this wavefield.

Subsequent polarization has nearly eliminated the downgoing SV from the longitudinal wavefield (fig 11). The strong direct P arrival is perturbed by high velocity reflected events at several points, indicated by five depth annotations on the aligned stacks in figure 12. Such disturbances are not observed on the horizontal axis nor on

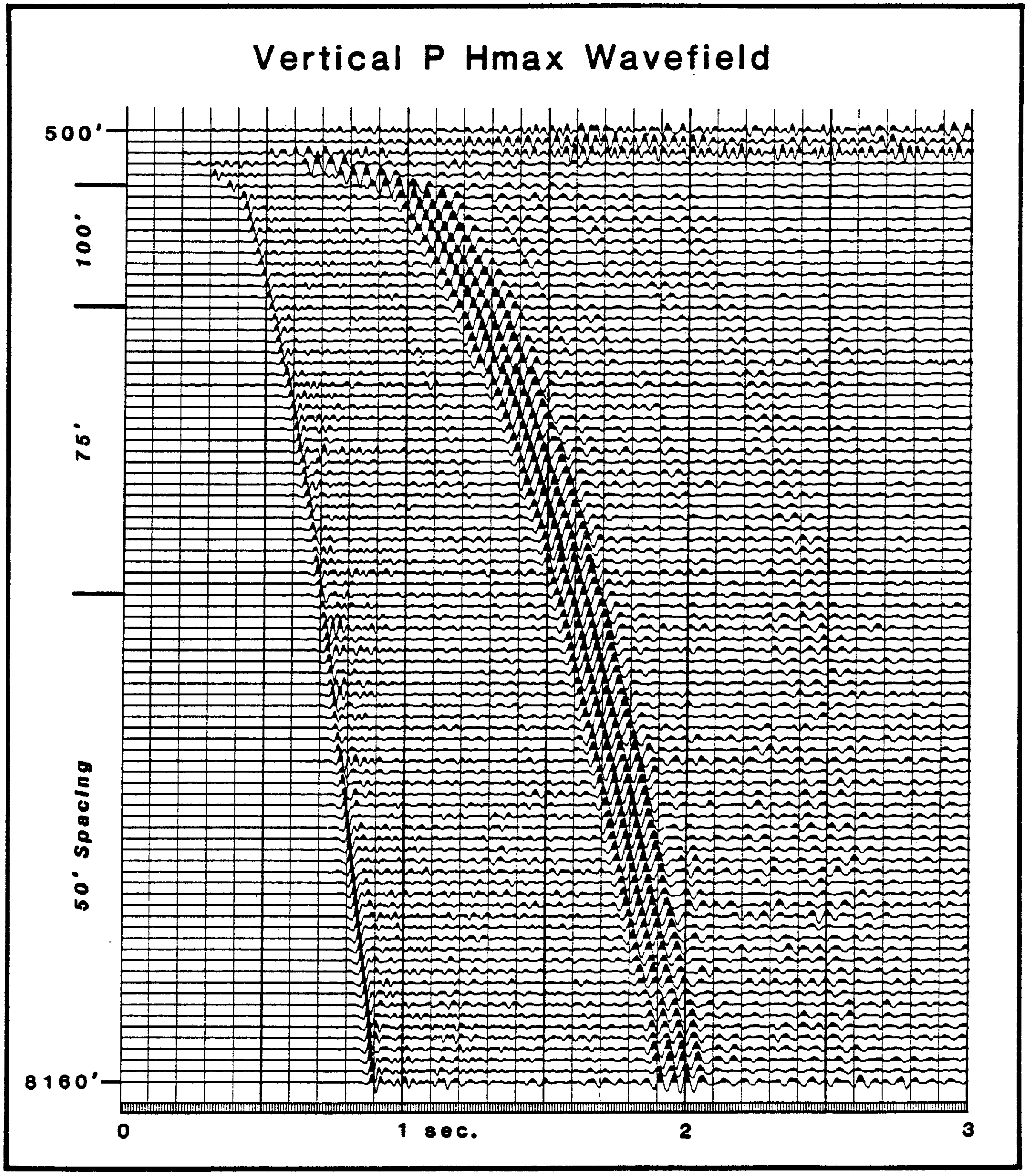

Figure 9. Polarized data from the P-wave vibrator, 400 ft offset. Hmax is the axis of maximum horizontal motion. Depths where spacing changes are given in Table II.

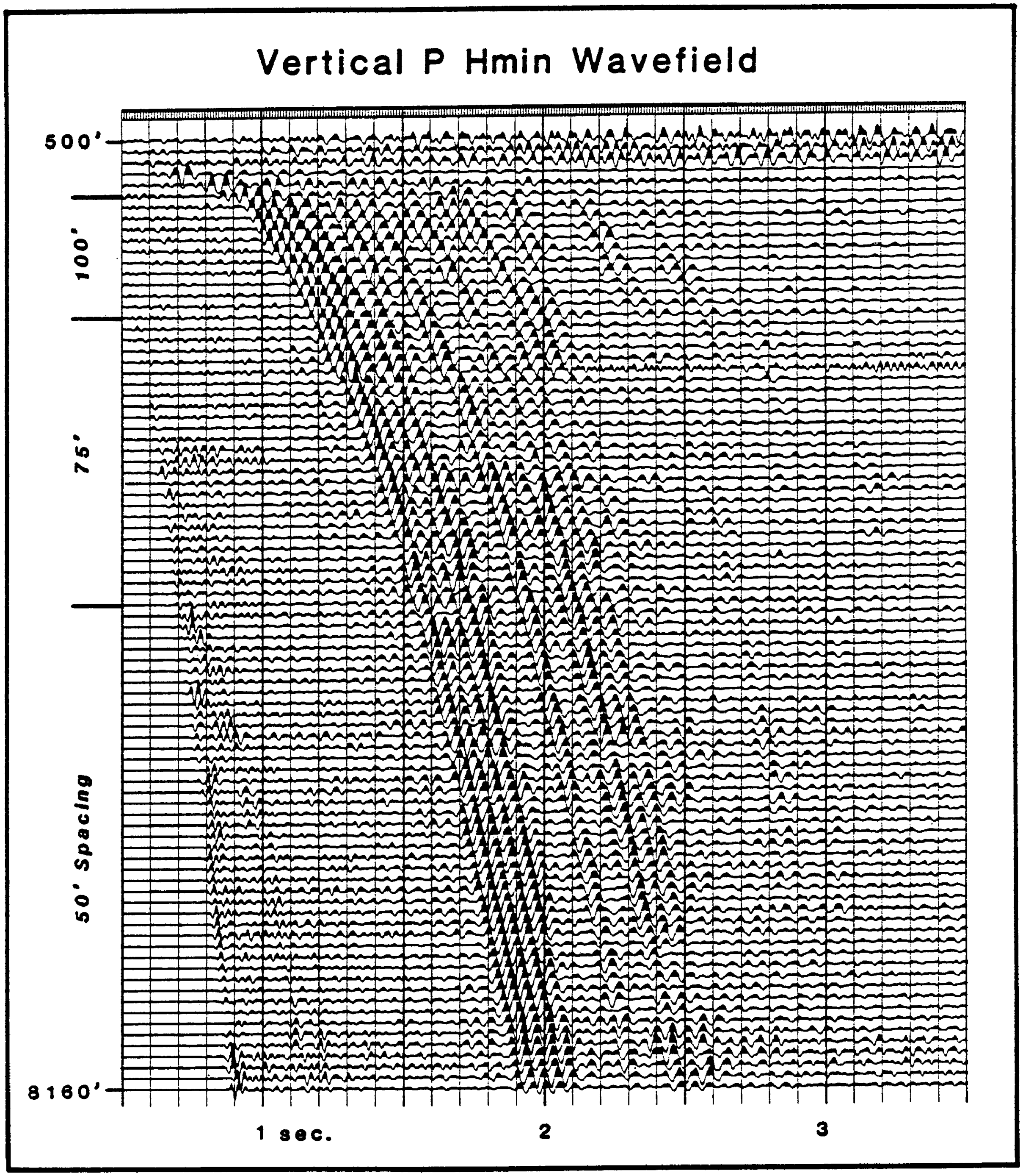

Figure 10. Polarized data from the P-wave vibrator, 400 ft offset. Hmin enhances out-of-plane SH waves.

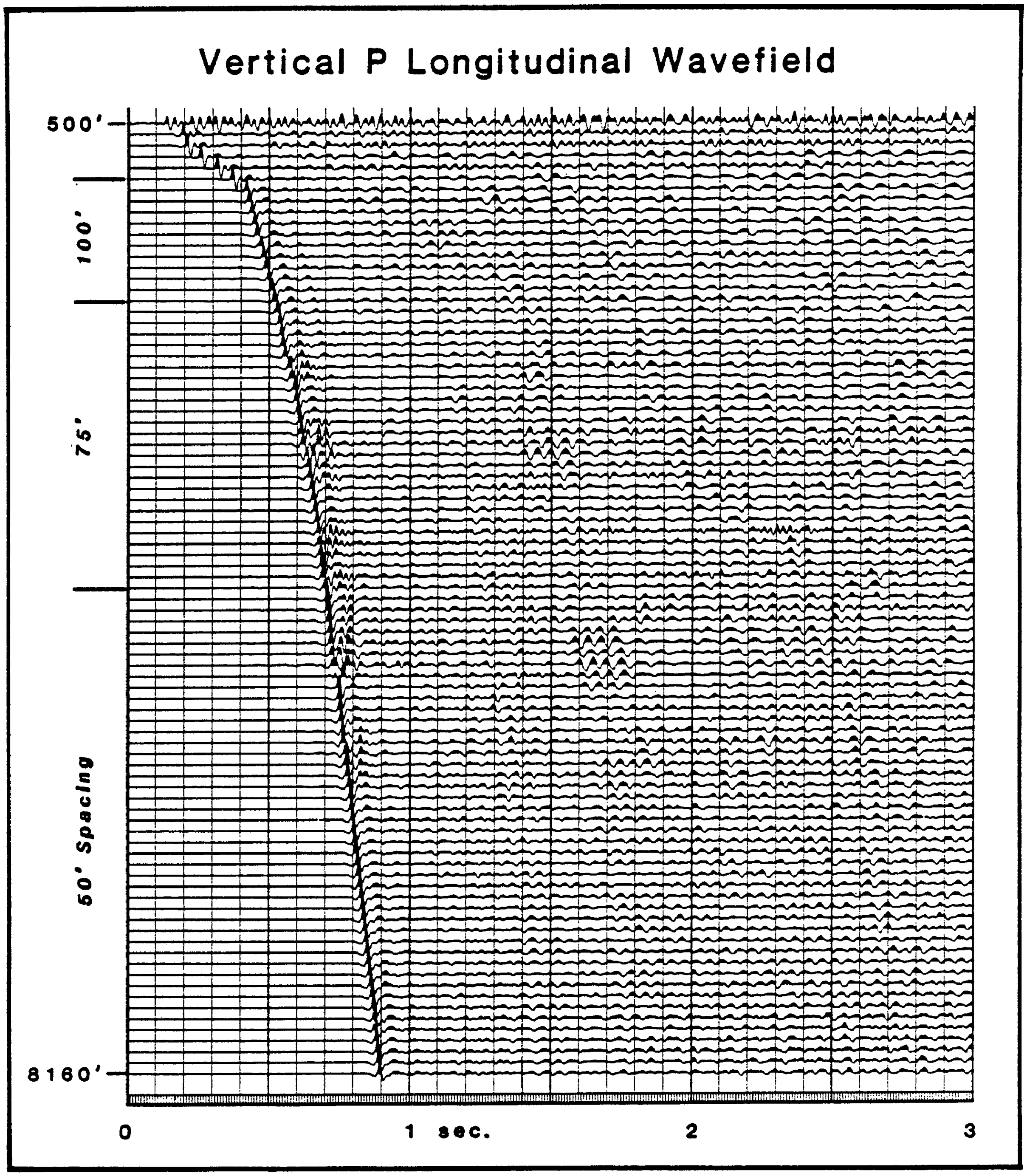

Figure 11. Polarized data from the P-wave vibrator, 400 ft offset. Longitudinal polarization enhances direct and reflected P-waves for this acquisition geometry.

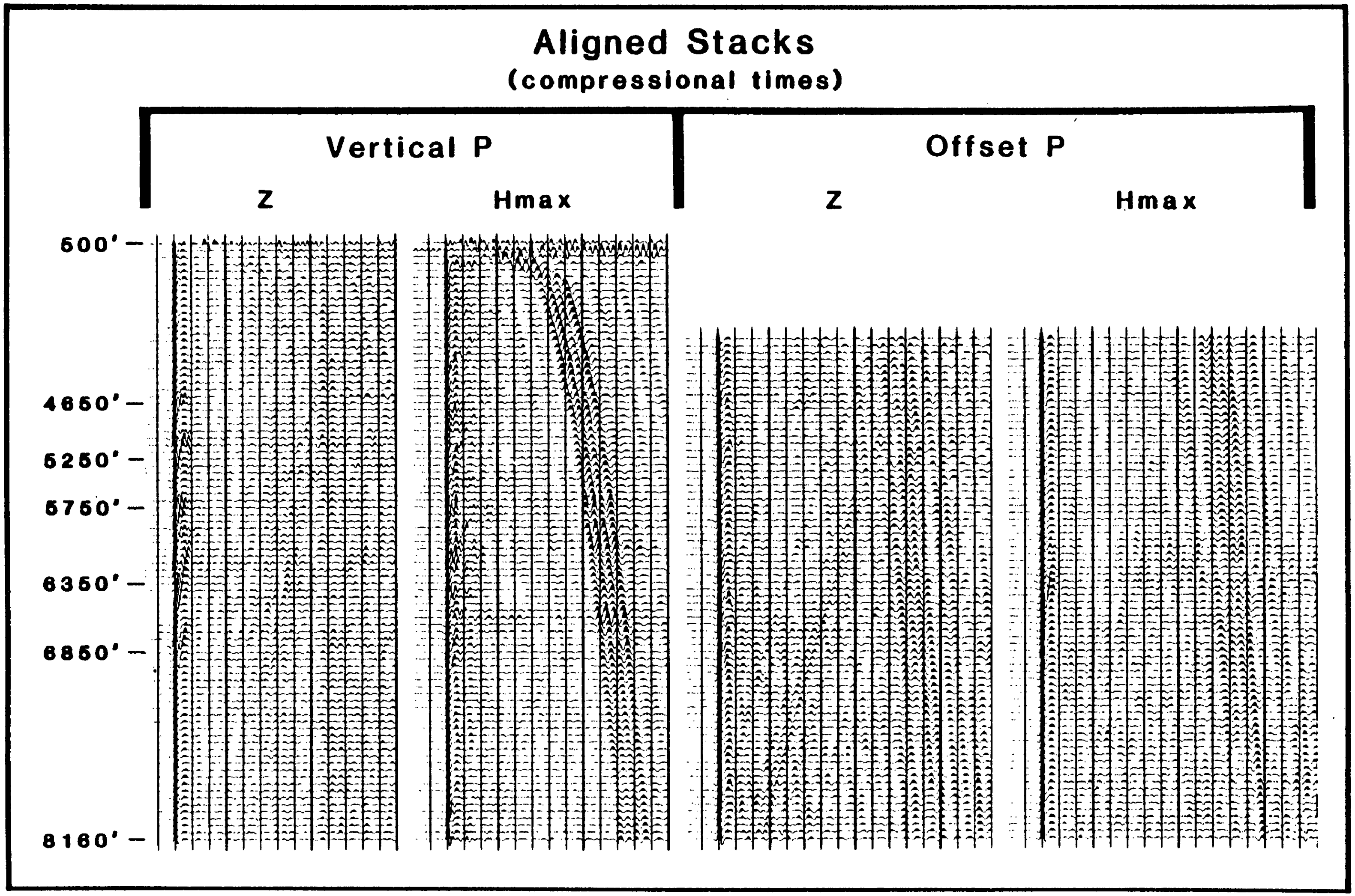

Figure 12. Strong casing reflections between 4650 and 6850 ft are not present on offset data.

either axis of the far offset. The velocity of these events appears to be 18,000 ft/sec, close to that of casing (17,500). These events are not from geologic interfaces, but possibly a water hammer effect as the P wave passes a restriction in the casing-formation annulus.

Transverse polarization (fig 13) has enhanced the downgoing SV, leaving only a weak P arrival. Converted shear reflections can be seen originating below TD at 1.17 sec and from the direct P arrival at 0.89 sec. A P-S-S reflection, originating from the direct shear arrival at 1.9 sec is visible by sighting along a shear reflection slope. Signal-to-noise ratio appears as good as that for the longitudinal result.

The shear vibrator produces a Hmax wavefield (fig 14) surprisingly clean before the first shear arrival. Low frequencies dominate a record containing good energy and no apparent compressional waves. The basic shear wavelet does not ring like that in the compressional record. Downgoing multiples are stronger than any observed in the P data. The vibrator was oriented to produce SH waves, thus Hmax should be 90 degrees from the P-SV plane.

Downgoing shear is weaker in the Hmax wavefield of the 4500 ft offset compressional vibrator (fig 15) than that observed from the vertical source. As in the vertical

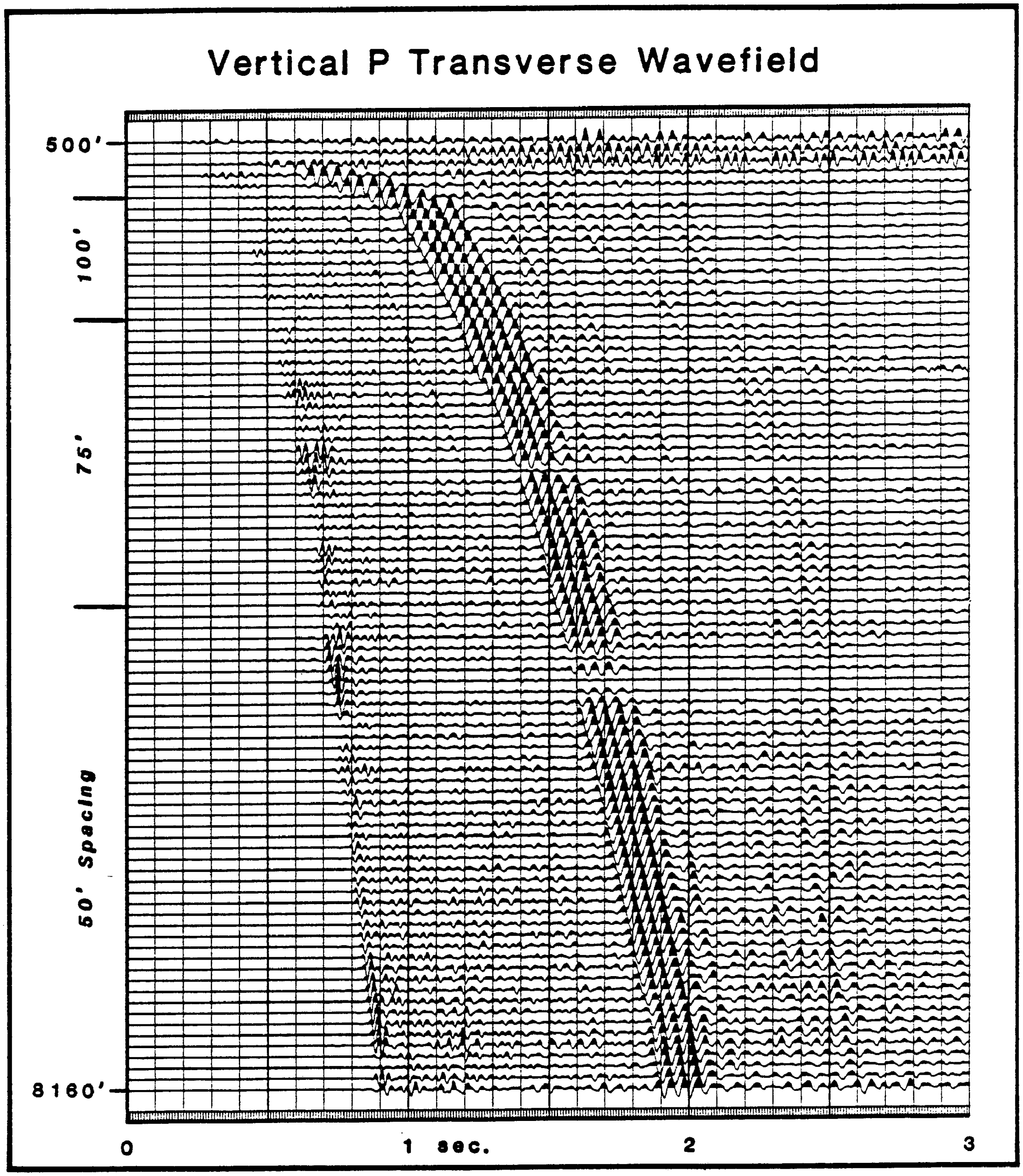

Figure 13. Polarized data from the P-wave vibrator, 400 ft offset. Transverse polarization enhances direct and reflected SV-waves for this acquisition setup.

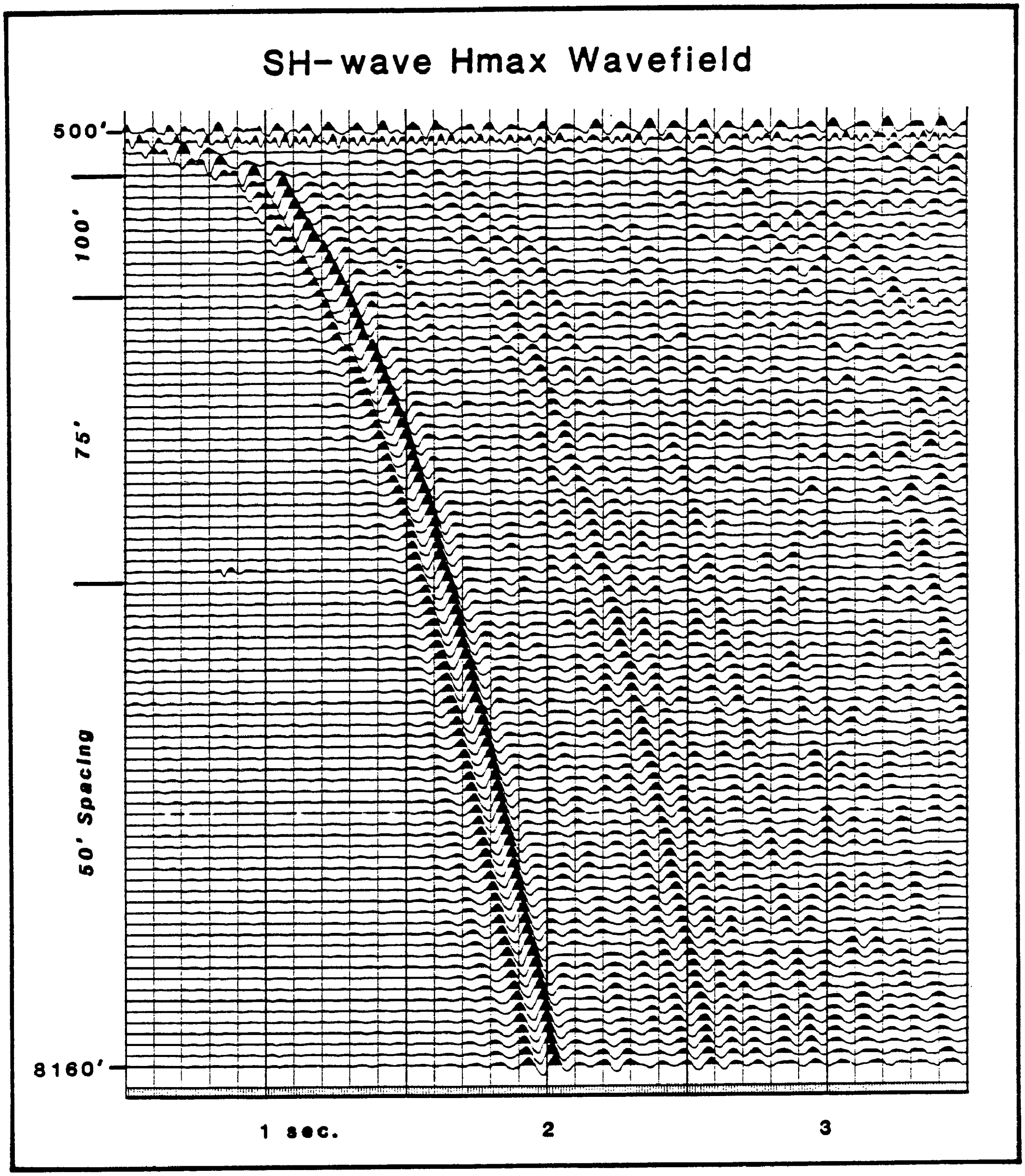

Figure 14. Polarized data from the SH-wave vibrator, 400 ft offset. Hmax represents the axis of maximum horizontal motion.

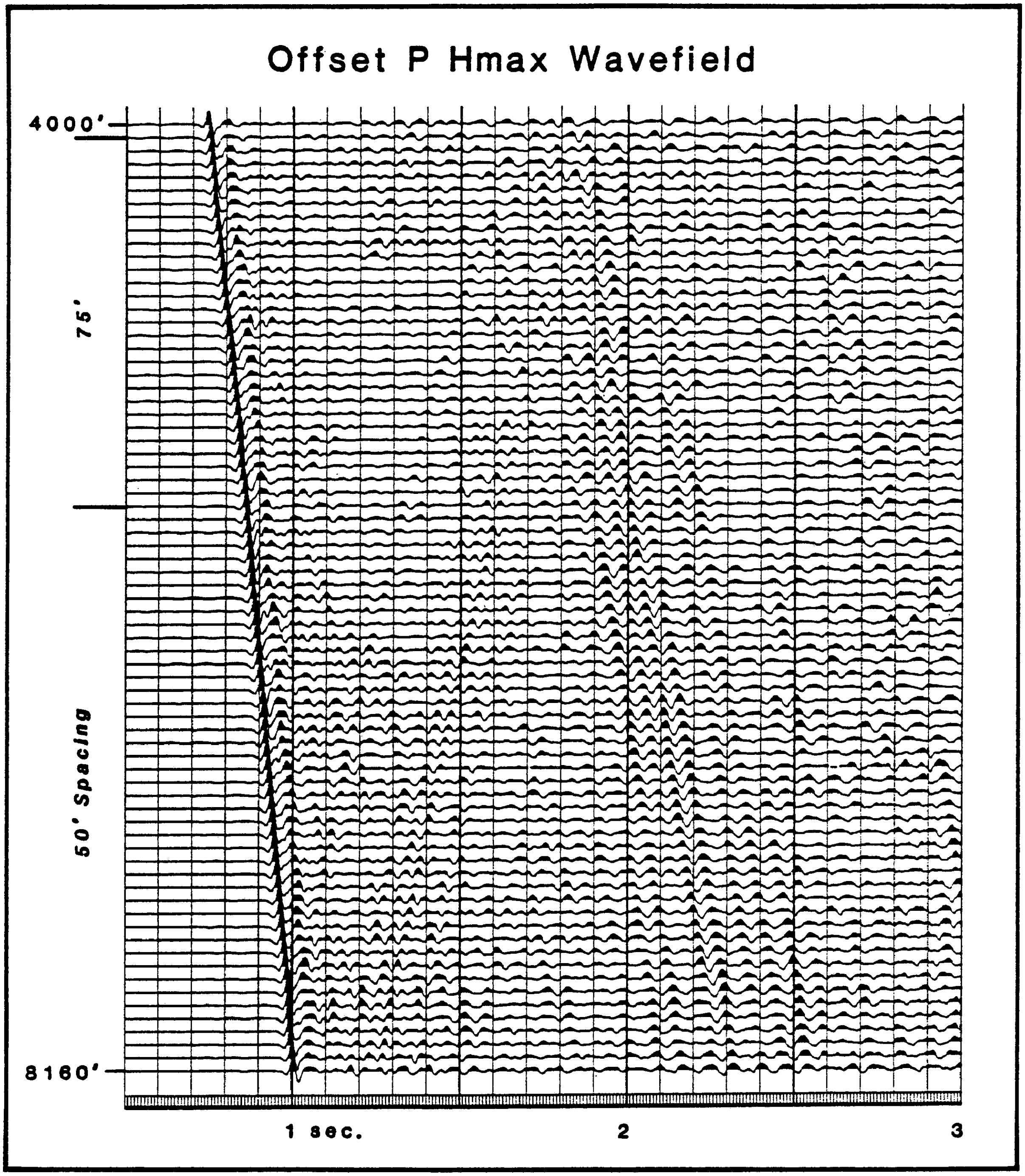

Figure 15. Polarized data from the P-wave vibrator, 4500 ft offset. Hmax represents the axis of maximum horizontal motion.

source records, the strong P arrival contrasts with the indistinct event in the Hmin wavefield (fig 16). Hmin has an apparently stronger shear arrival, but poorer signal-to-noise ratio.

Offset longitudinal and transverse polarizations (figs 17,18) produced only one surprise. Both upgoing compressional and shear reflections can be clearly seen when sighting along the transverse results. This polarization should have enhanced the P reflections, but the converted shear events are stronger. Transmitted P-SV conversions, originating at the direct P arrival, can be seen on the transverse wavefield (eg 0.85 and 0.90 sec).

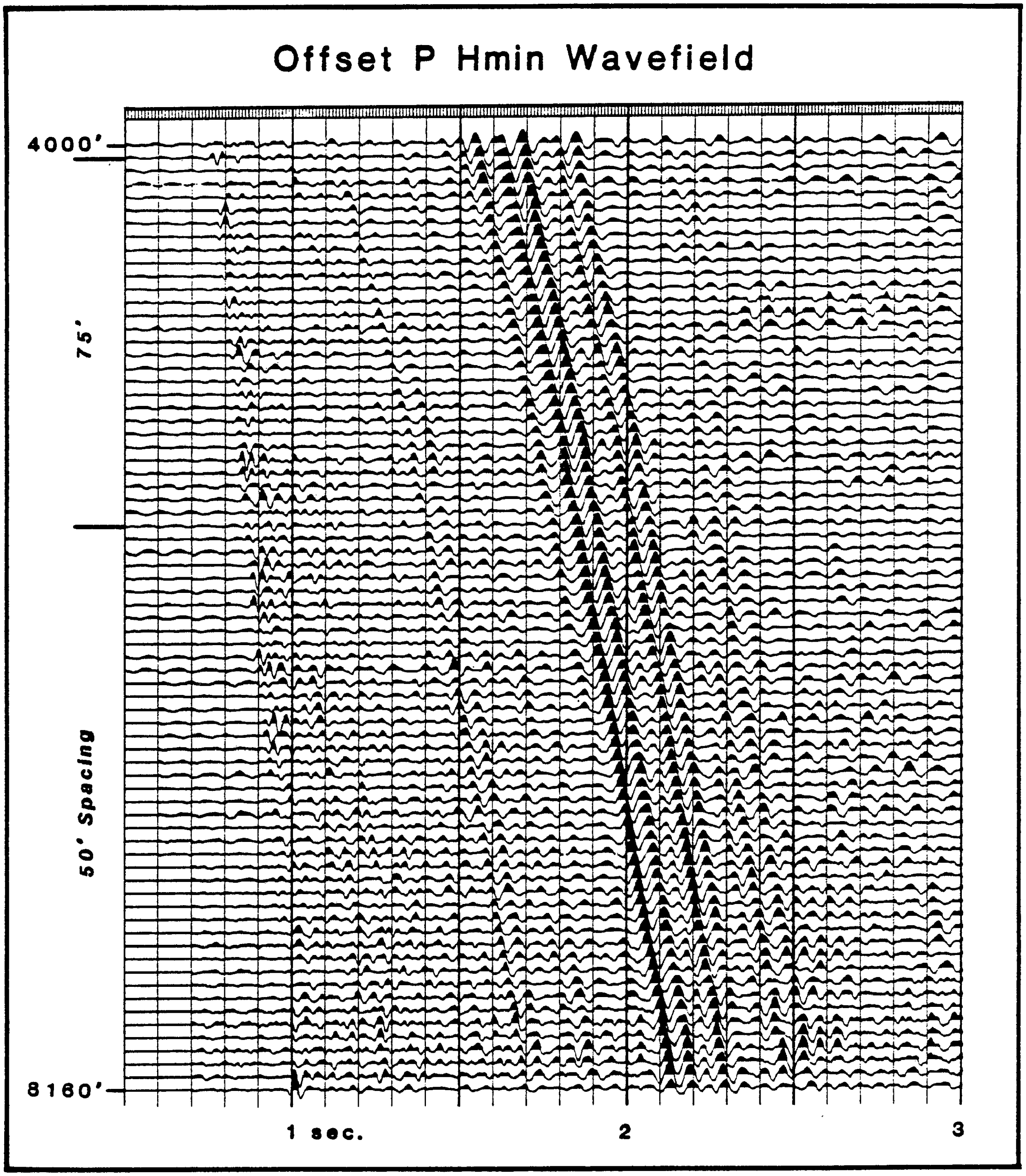

Figure 16. Polarized data from the P-wave vibrator, 4500 ft offset. Hmin enhances out-of-plane SH motion.

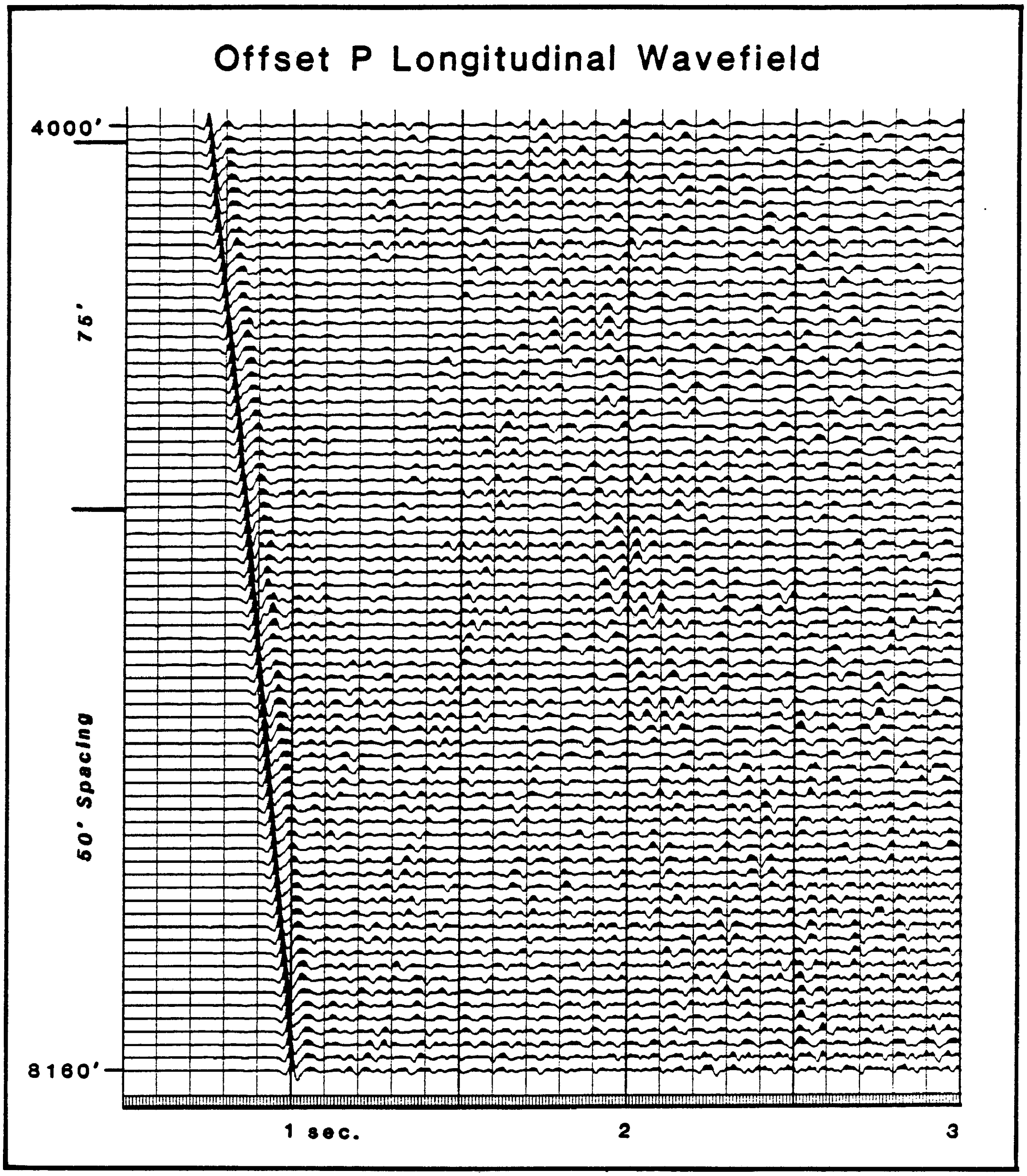

Figure 17. Polarized data from the P-wave vibrator, 4500 ft offset. Longitudinal polarization enhances direct P- and reflected SV-waves for this acquisition setup.

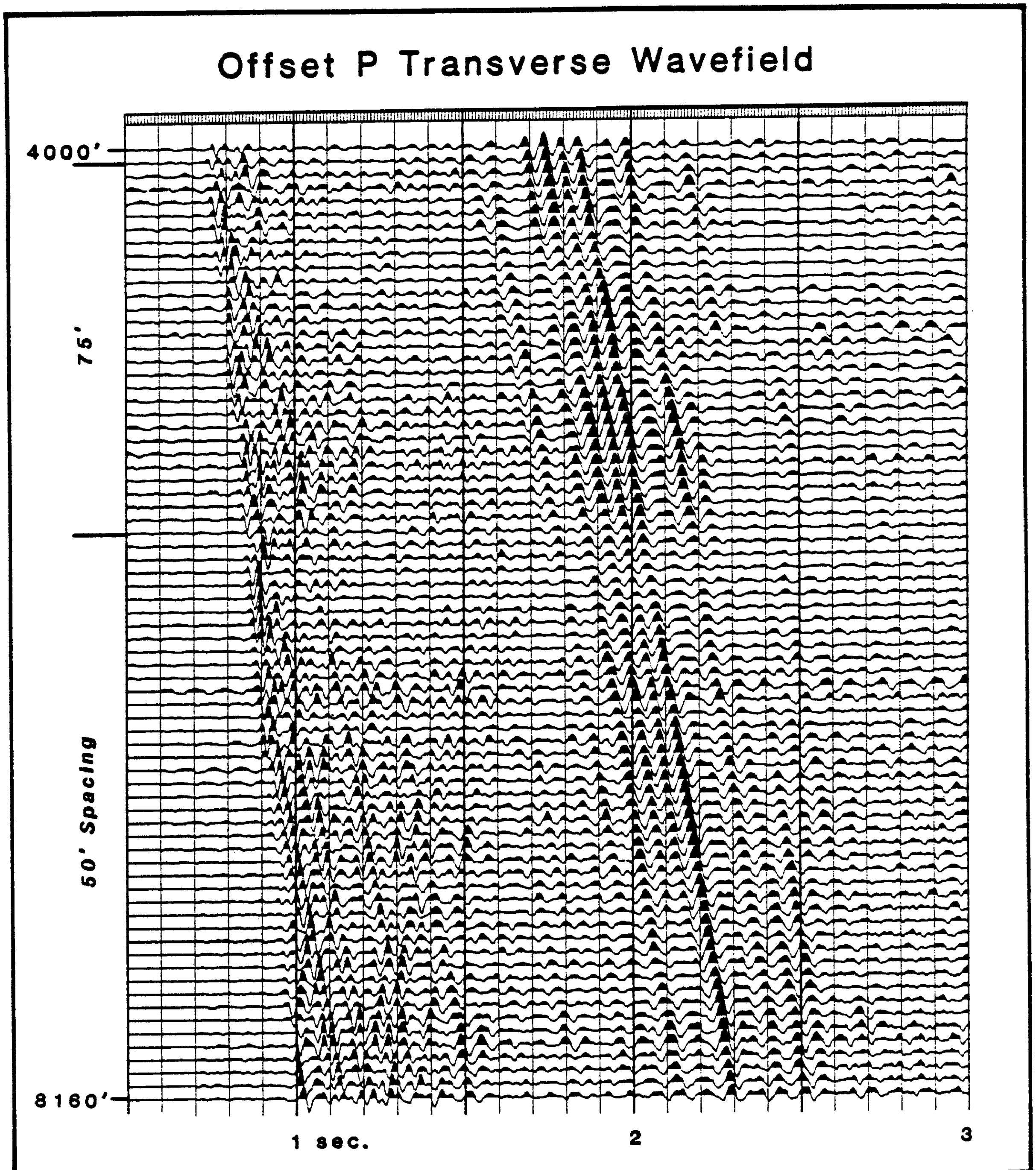

Figure 18. Polarized data from the P-wave vibrator, 4500 ft offset. Transverse polarization enhances direct SV- and reflected P-waves for this acquisition setup.

MODELING

Models from the velocity logs help understand why both P and S reflections are observed on the offset transverse wavefield. Figs 19,20 and 21 show ray trace results for direct arrivals, P-P and P-S reflections from the top of the Niobrara formation, generated using the model in Table III. Direct arrival times predicted by the model agree with those observed from the VSP data within +/- 2 ms, lending credibility to modeled raypaths.

Table III also lists amplitudes and angles of incidence to the well for a tool positioned at 6850 ft and reflections from the top of the Niobrara for various source offsets. From the model, the vertical reflection coefficient of this interface is 0.109 for P waves and 0.166 for S waves. Modeled reflection amplitudes are 10% of incident and shear values are larger than P, both decreasing with offset.

In contrast, the converted wave reflection amplitude increases with offset, starting at less than 2% of the direct P amplitude and increasing to nearly 10% for the 4500 ft offset. The converted reflection is nearly twice as large as the P-P reflection at the far offset. This effect is compounded by differences in the incident

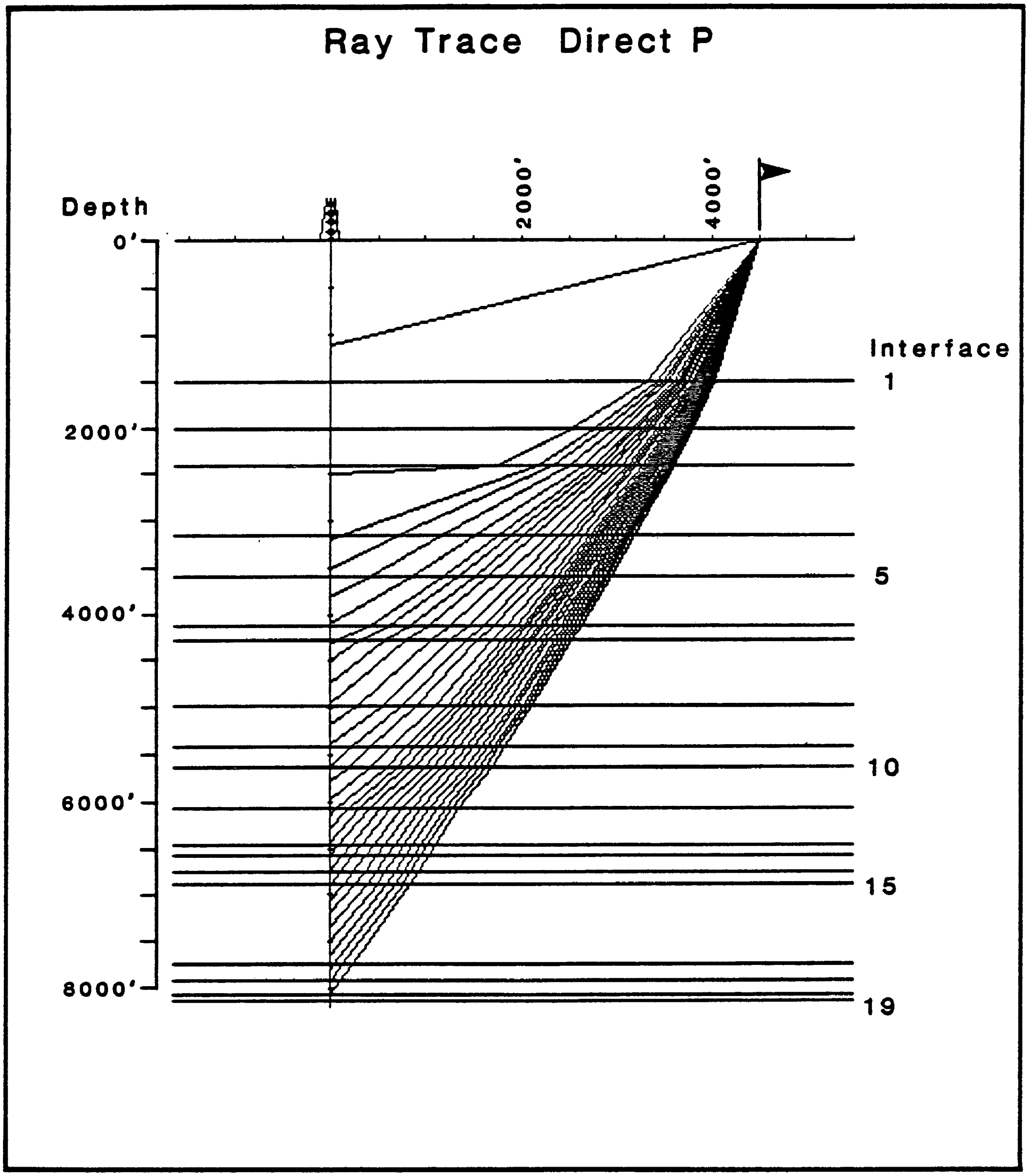

Figure 19. Direct arrival raypaths for 4500 ft offset from the model of Table III.

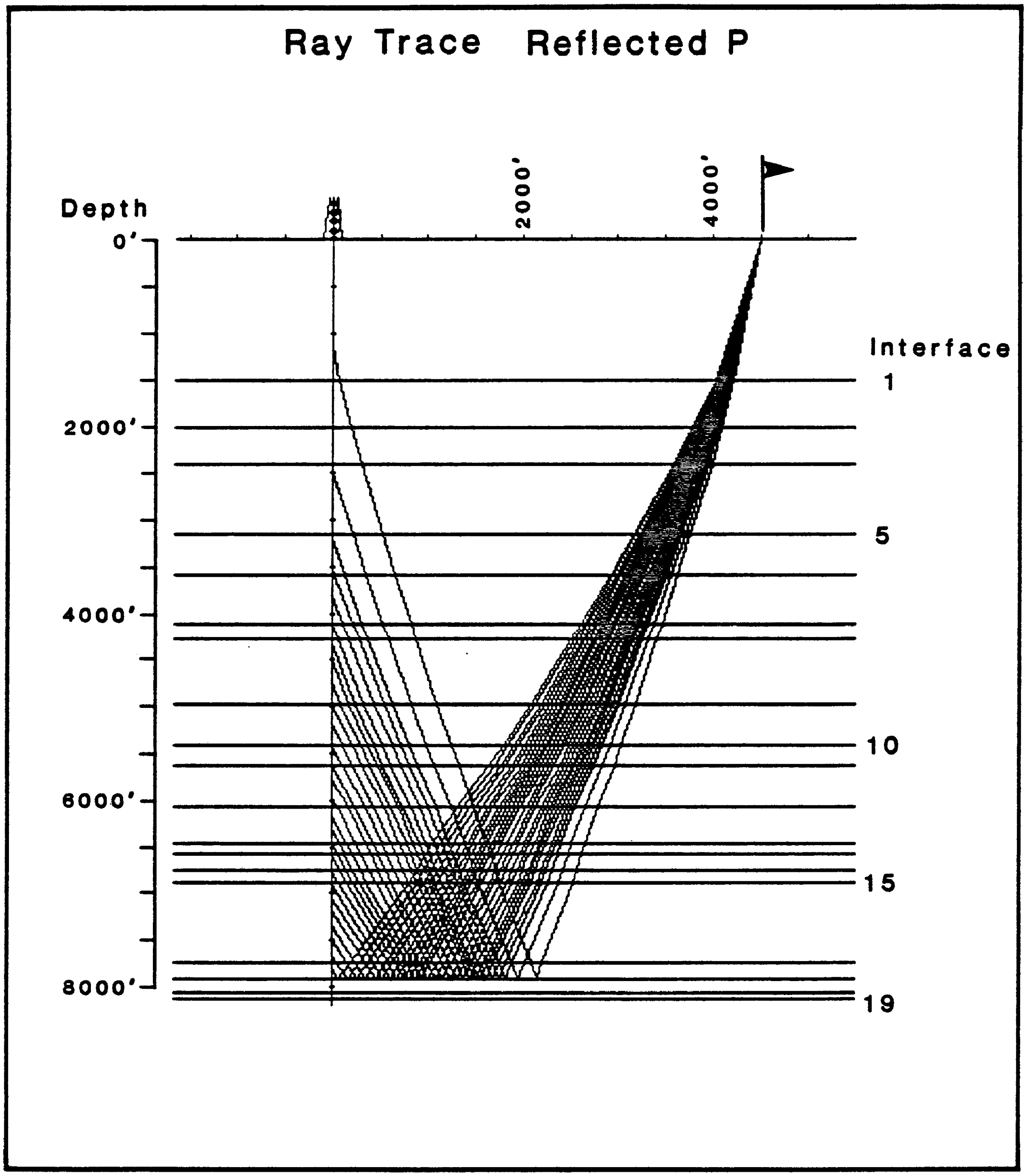

Figure 20. Compressional raypaths reflected from the top of Niobrara for 4500 ft offset from the model of Table III.

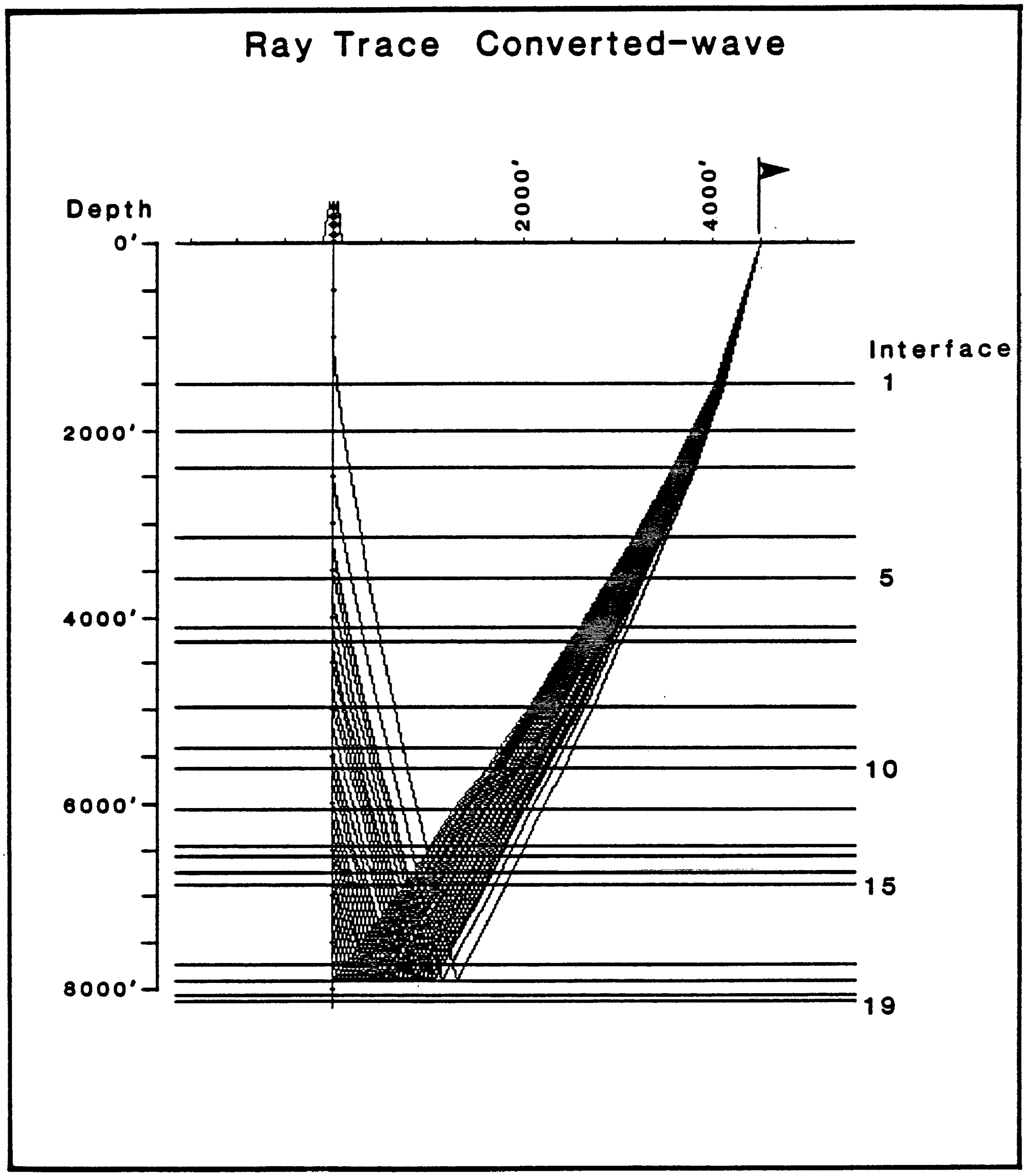

Figure 21. Raypaths of converted P-SV reflections from the top of Niobrara for 4500 ft offset from the model of Table III.

TABLE III

MODEL FROM VELOCITY LOGS

Layer	Depth (top)	V_p (ft/sec)	V_s (ft/sec)
1	0	6045	2558
2	1500	8320	3670
3	2010	8772	4084
4	2400	9824	4565
5	3150	9667	3958
6	3600	10162	4988
7	4122	11151	5441
8	4275	10121	5079
9	4975	11239	5958
10	5415	10728	5360
11	5633	12137	5956
12	6080	10763	5465
13	6468	9790	4937
14	6585	11073	5926
15	6745	10471	5130
16	6875	11716	5910
17	7730	10475	5135
18	7920	13060	7172
19	8060	11984	6481
20	8137	13178	7197

Depth 6850	AMPLITUDES				ANGLE OF INCIDENCE to geophone			
Wave	400	1500	3000	4500	400	1500	3000	4500
up P	.080	.075	.062	.048	2	10	18	27
up S	.109	.082	.073	.061	2	10	18	27
up P-S	.013	.046	.079	.091	1	5	10	14
down P	.740							
down S	.676				176	165	153	143

angles to the geophone.

Returning to figures 19, 20 and 21, comparison of direct and reflected raypaths indicate the P-P and S-S polarizations are essentially correct, since the offset survey only covers the lower half of the well. Polarization of the P-S reflections are not accurate, hence both longitudinal and transverse wavefields would be expected to contain some reflected shear energy.

F-K PLOTS

F-K plots of final polarization results support the observations made of the wavefields. Average compressional velocity is 11450 ft/sec while shear velocity averages 5790 ft/sec on these plots.

In the vertical P data, P energy has been enhanced in the longitudinal record (fig 22) but traces of shear energy are still present. The upper frequency limit for this data is approximately 50 Hz. Harmonics of the 15 Hz noise from nearby production pumps appear along the frequency axis. 12 Hz noise and the 24 Hz harmonic have not been explained.

In contrast, considerably more than a trace of P energy remains in the transverse axis (fig 23). Polarization does not reject signal, but merely tends to enhance various wave modes. Thus for a compressional source, the observed result should not be surprising. When compared to the longitudinal results, shear has been considerably enhanced, dominating below 25 Hz.

The low frequency character of the vertical SH data is glaringly evident in the F-K plot of figure 24. Energy is essentially restricted to the 6-16 Hz range.

The offset longitudinal data (fig 25) contains

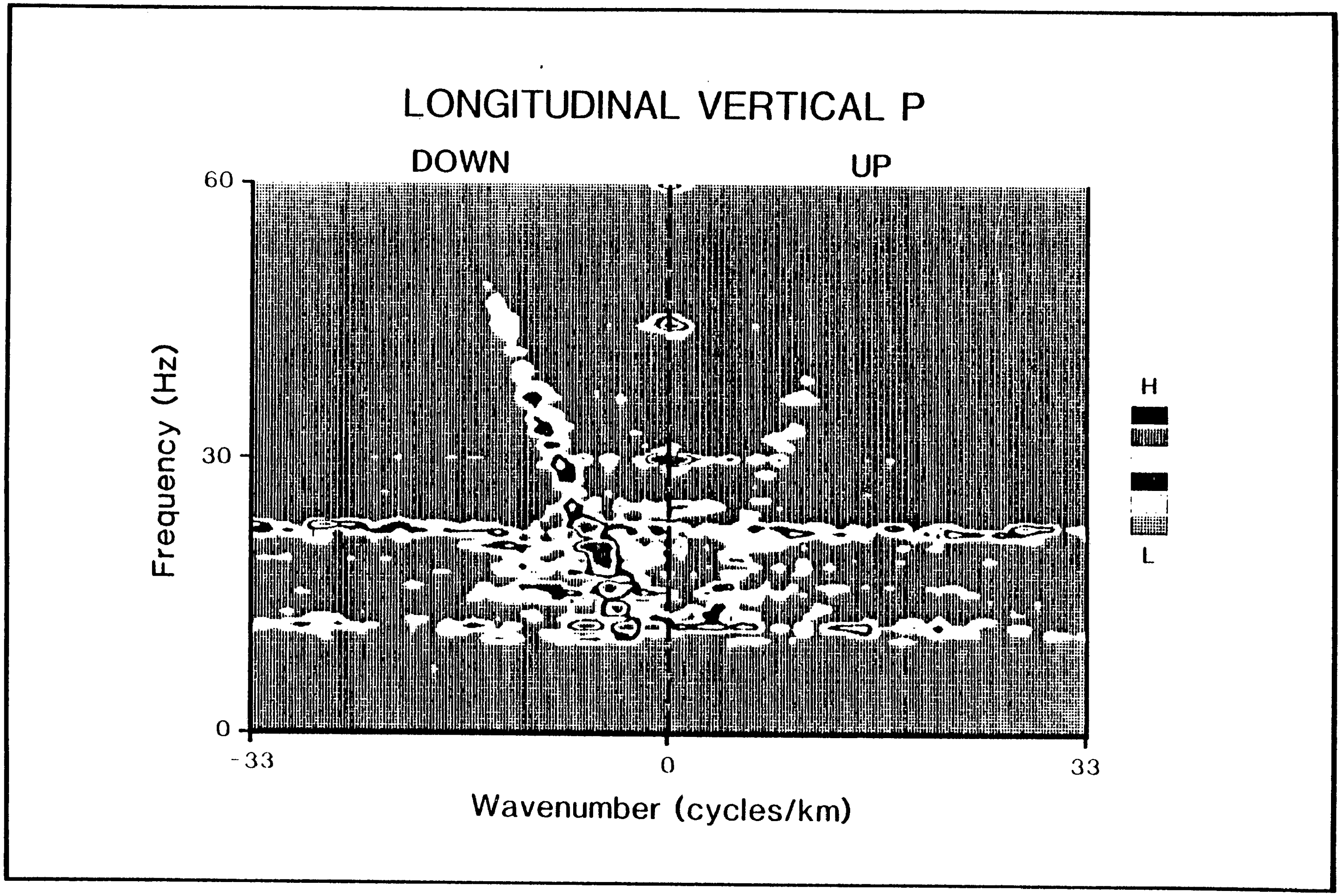

Figure 22. F-K plot of the longitudinal wavefield from the P-wave vibrator, 400 ft offset. P energy is enhanced and only a trace of shear remains.

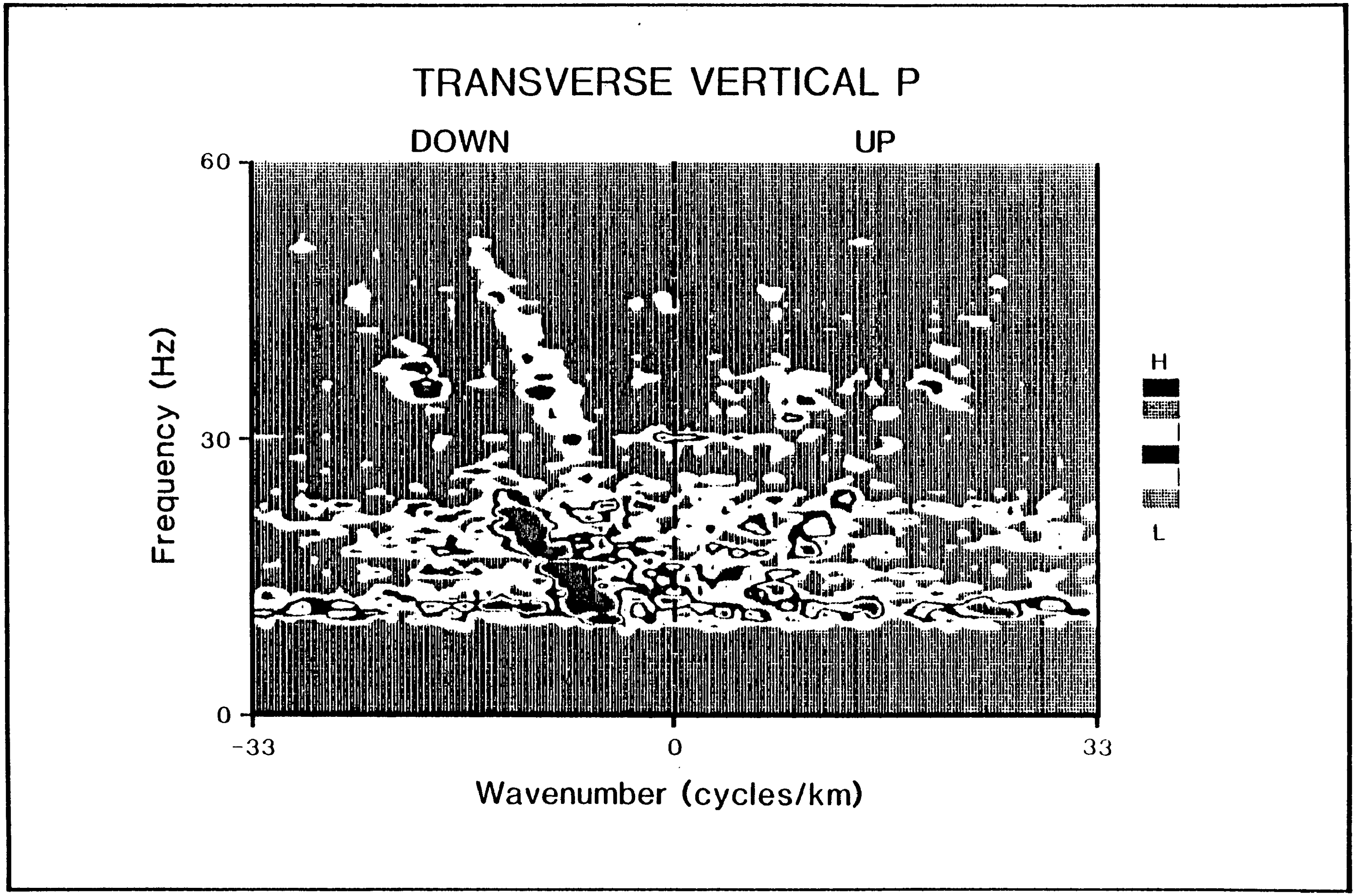

Figure 23. F-K plot of the transverse wavefield from the P-wave vibrator, 400 ft offset. Converted shear energy has been enhanced.

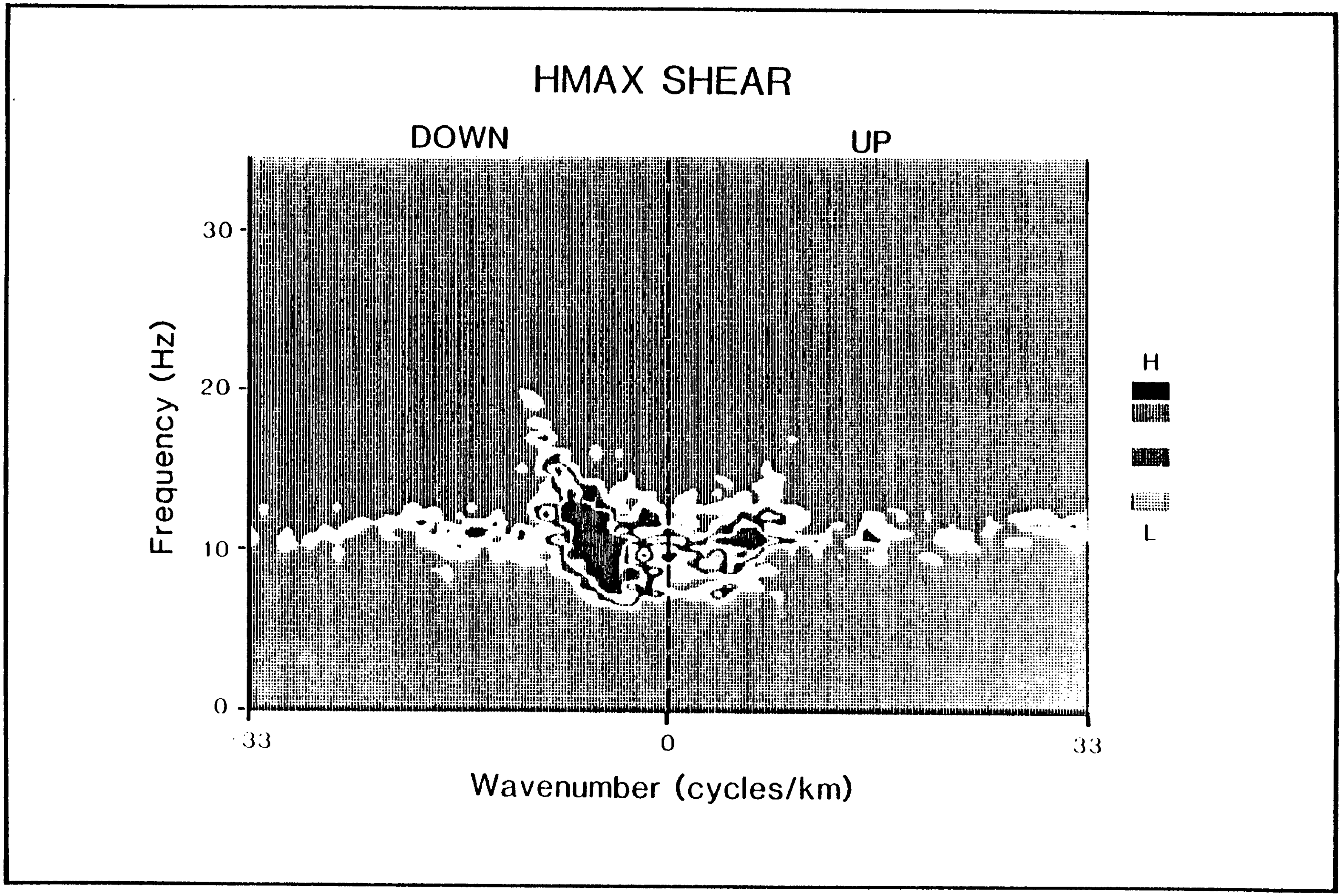

Figure 24. F-K plot of the Hmax wavefield from the SH-wave vibrator, 400 ft offset.

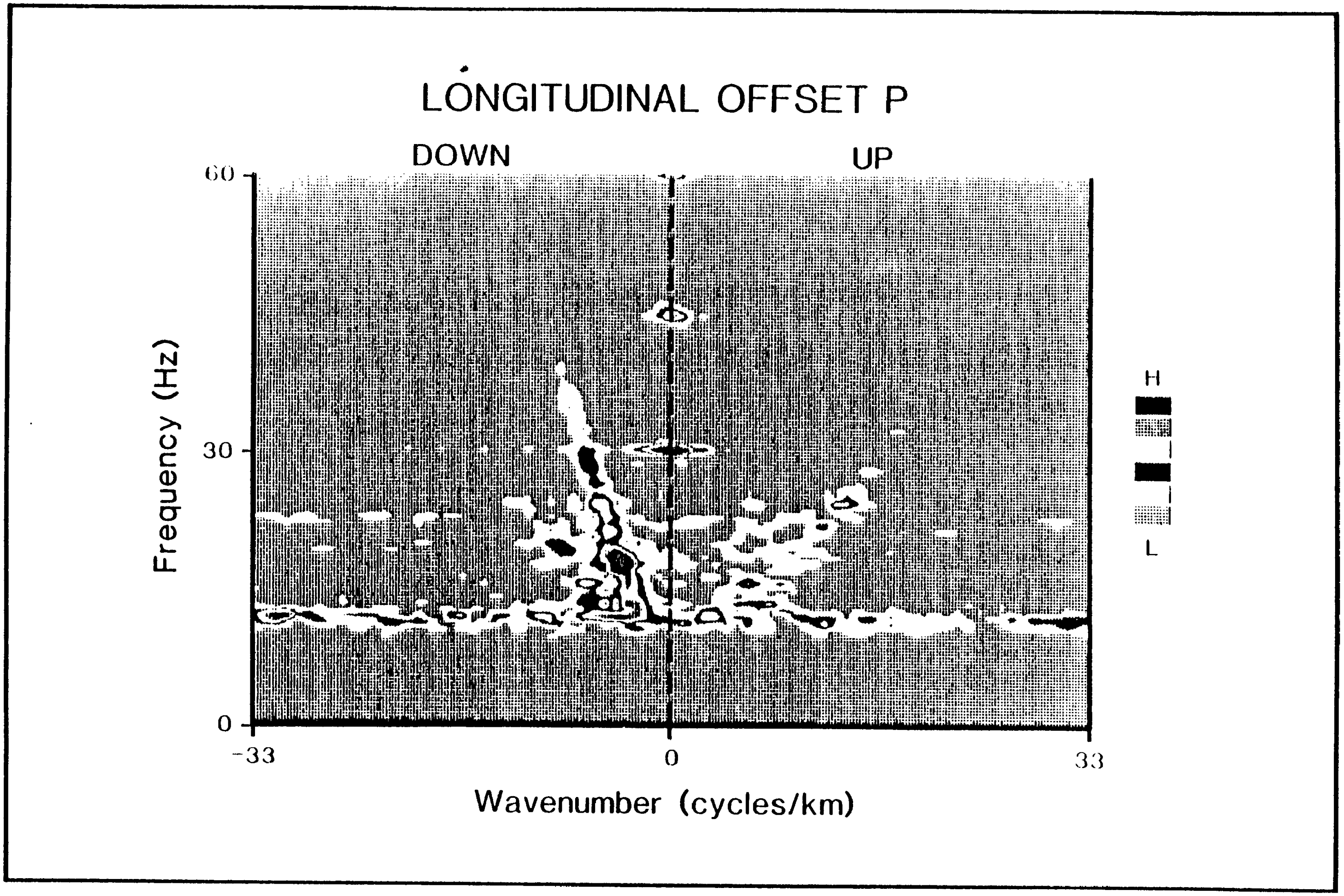

Figure 25. F-K plot of the longitudinal wavefield from the P-wave vibrator from the 4500 ft offset. Direct P and reflected SV energies are enhanced.

primarily downgoing P and upgoing shear. Traces of other modes are present but relatively weak. The upper frequency limit is slightly lower than that of the vertical survey and 15 Hz harmonics are again visible.

The offset transverse F-K plot (fig 26) displays downgoing shear with both upgoing P and shear. The reflected shear is stronger than the P events. This reflected shear has been noted on the data as converted P-S events and should not be dominant in this wavefield. Raytrace modeling indicated these events could appear and would be stronger than reflected P.

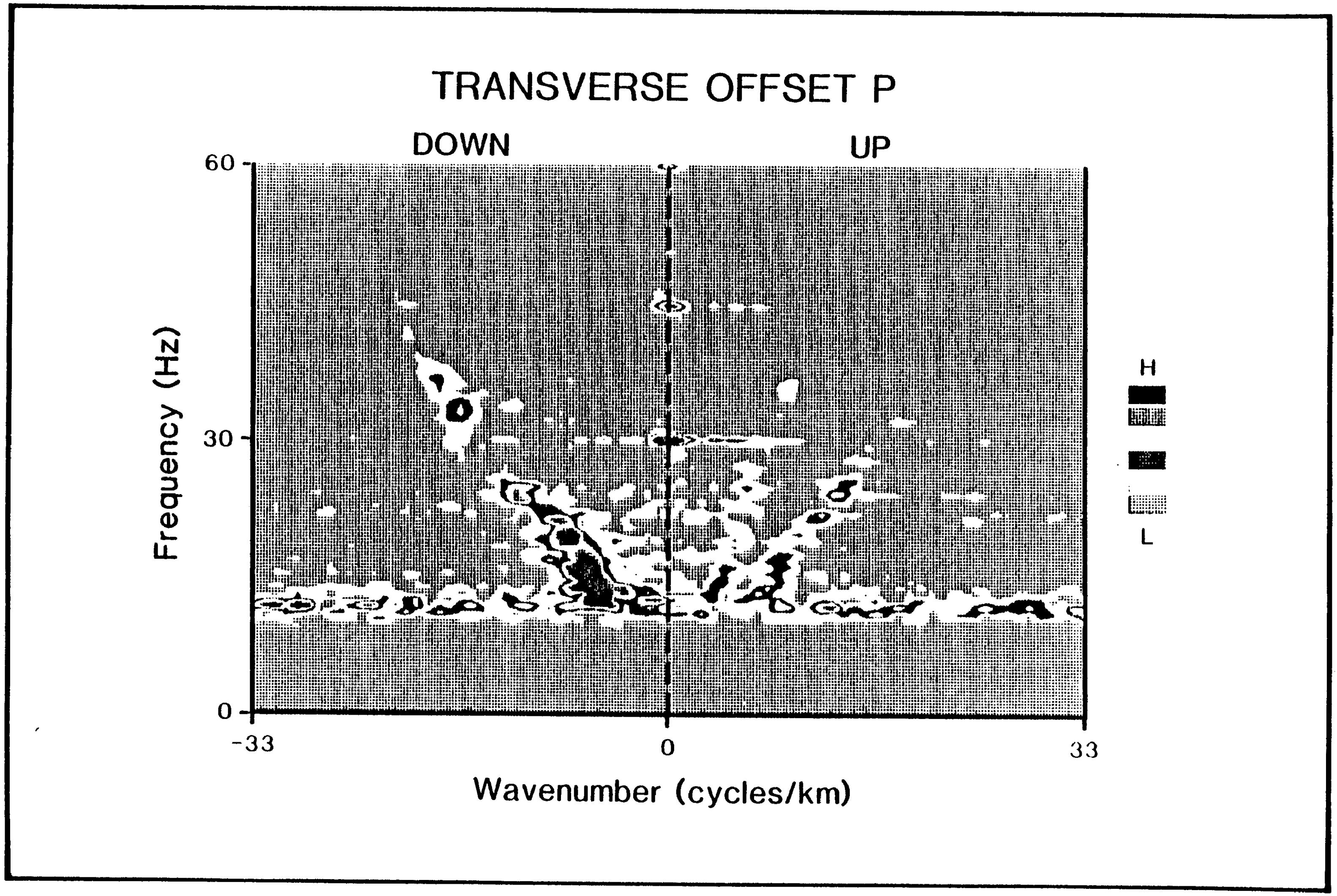

Figure 26. F-K plot of the transverse wavefield from the P-wave vibrator, 4500 ft offset. Direct SV and reflected P is enhanced. Some SV energy remains.

RESULTS

Using the appropriate polarized wavefields, processing proceeds as for the classical single component VSP for vertical P, vertical SH and offset P (Table IV). Wavefields were F-K filtered to remove compressional energy before attempting to extract shear reflections from the P-source data. Deconvolution of converted wave results proved difficult.

All reflected results are processed through wave-shaped deconvolution and presented in two way time without AGC. Moveout correction of offset data is done after deconvolution. Corridor Stacks use only the first 200 ms after the direct arrival from each trace, retaining the entire length of the bottom seven traces.

Standard Processing

Good continuity and little noise characterize the vertical P results (fig. 27). Dimming of reflections when passing behind a strong shallower reflector (eg. reflections of 1.75-1.8 sec as they pass events at 1.6 or 1.3 sec) is typical of VSP displays without AGC. Several traces have been deleted before velocity filtering in an attempt to remove the influence of the casing reflections

TABLE IV

VSP PROCESSING CHAIN

Load / Demux

Vertical Stack - manual rejection of bad traces
median stack

Break picks - verified interactively

Polarization

input	output
X, Y axes	Hmax - in-plane SV wave
	Hmin - uncoupled SH wave
Z, Hmax axes	longitudinal - direct P, refl. SV
	transverse - refl. P, direct SV

hodograms, angles, correlation coefficients for quality control

Bandpass filtering - 6-70 Hz , third order Butterworth

F-K filter - manual rejection of P energy before shear processing, not performed on SH source

Gain correction - $(T/T_o)^{1.4}$

Time-domain velocity filter - 9 level for P and SH
11 level for shear extraction

Waveshape Deconvolution - P 14-45 Hz, length 2.1 sec
shear 8-24 Hz, length 1.2 sec

Moveout correction - for offset source positions

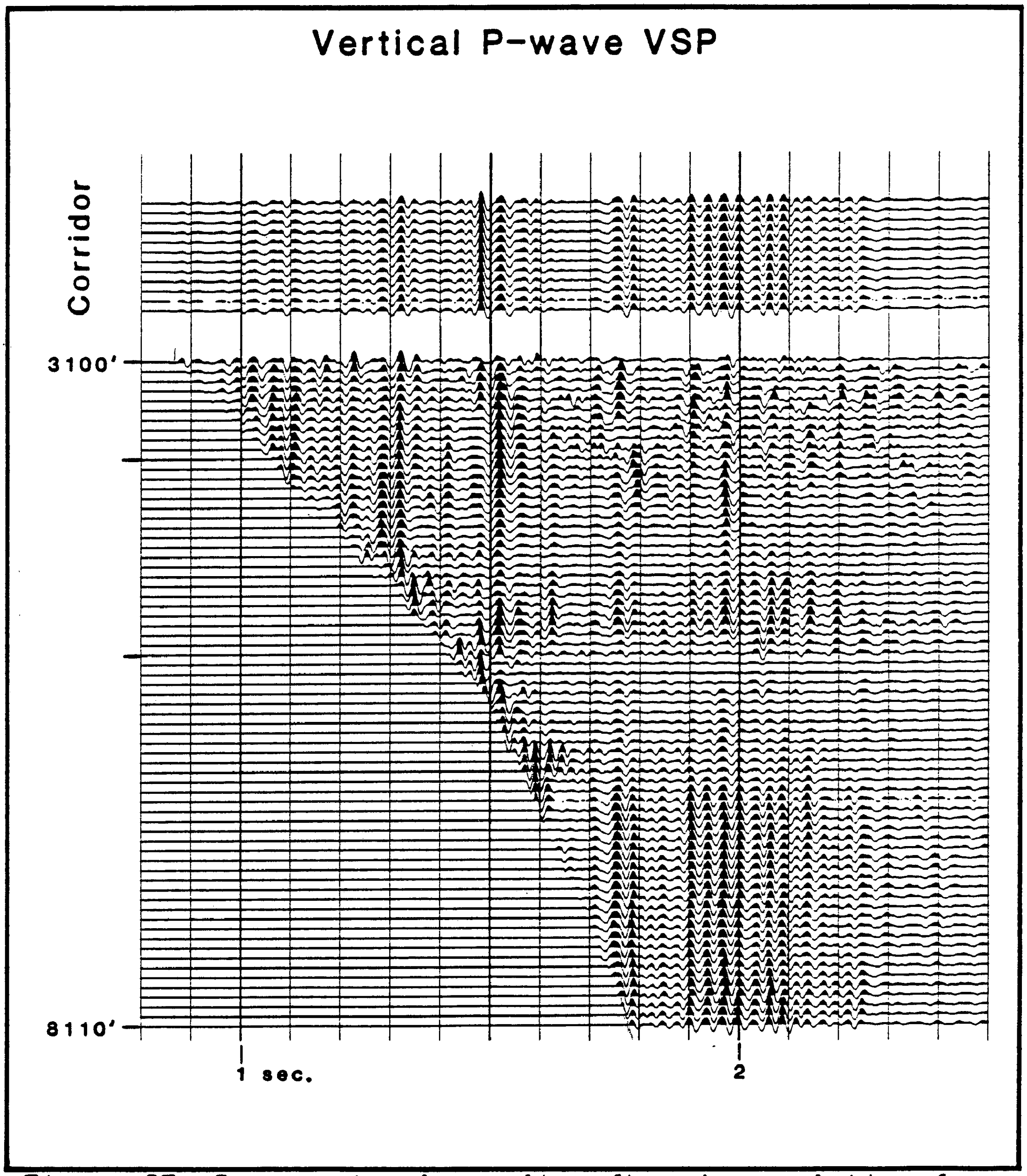

Figure 27. Compressional results after deconvolution from the P-wave vibrator, 400 ft offset. The casing reflection at 1.48 sec is not entirely removed.

noted earlier. This has not entirely succeeded at 1.48 sec, where the first arrivals and corridor stack are incorrect.

The vertical P result shows several perturbations of reflection alignment in the bottom 15 traces, particularly the event at 1.97 sec. Fracture and dip effects may be the cause. This effect can be seen on all reflection results.

The vertical SH results (fig 28) are noisier, though continuity of stronger reflections is still good. The deteriorated quality of the top four traces of this result appears to be due to formation anisotropy. (see Appendix C).

Figure 29 is a comparison of P and SH corridor stacks, synthetics and acoustic impedances. The shear displays are plotted at one half the time scale of compressional data and tied at the Niobrara reflection (1.77 sec P time and 3.83 sec shear). Events above and below will only match when the V_p/V_s ratio remains close to 2.0. The event and character match of both corridor stacks with the P synthetic is remarkable. The strong event at 1.48 sec on the compressional corridor stack is due to incomplete removal of a casing reflection.

The P synthetic has been convolved with a 27 Hz

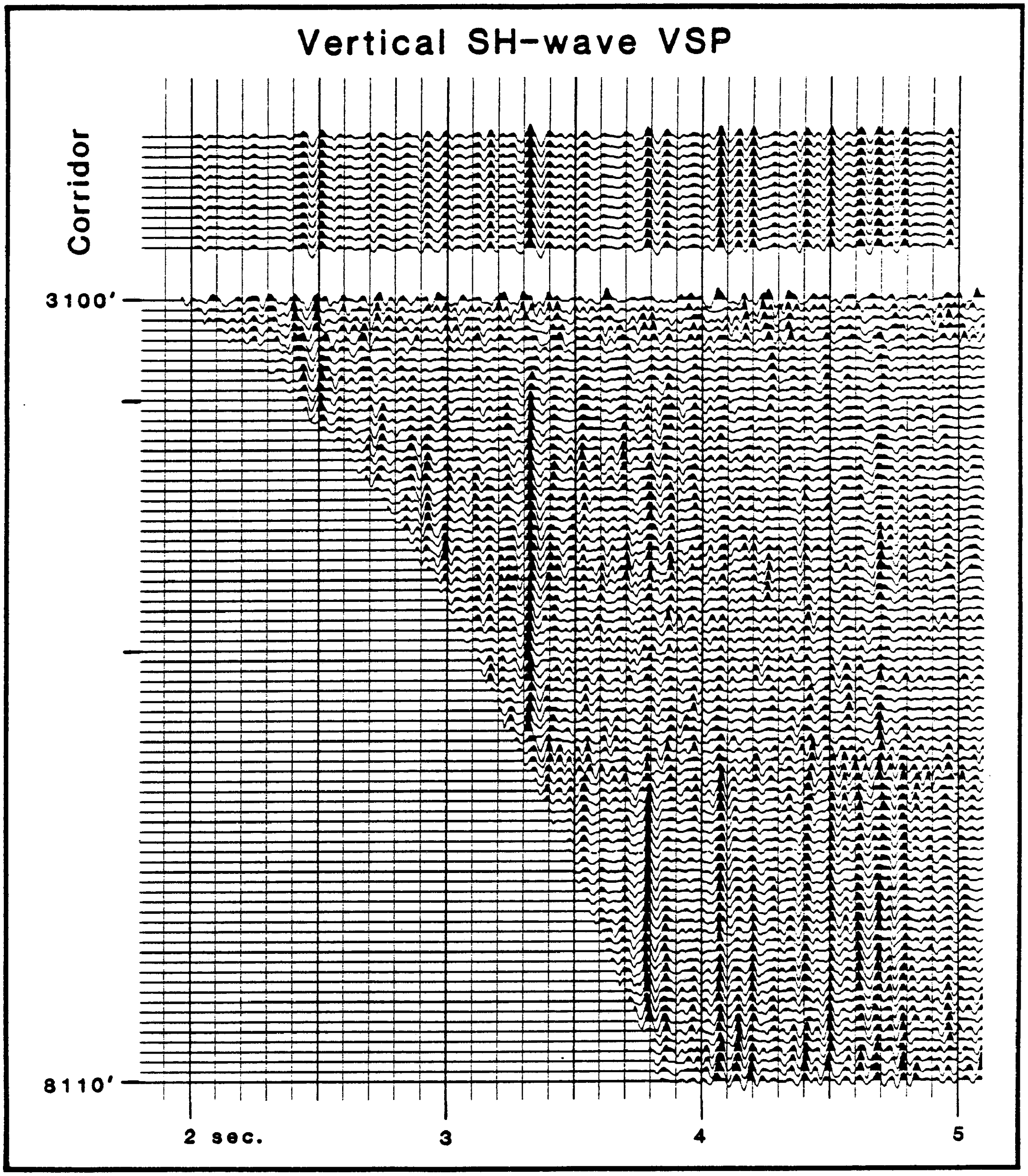

Figure 28. Shear results after deconvolution from the SH-wave vibrator, 400 ft offset.

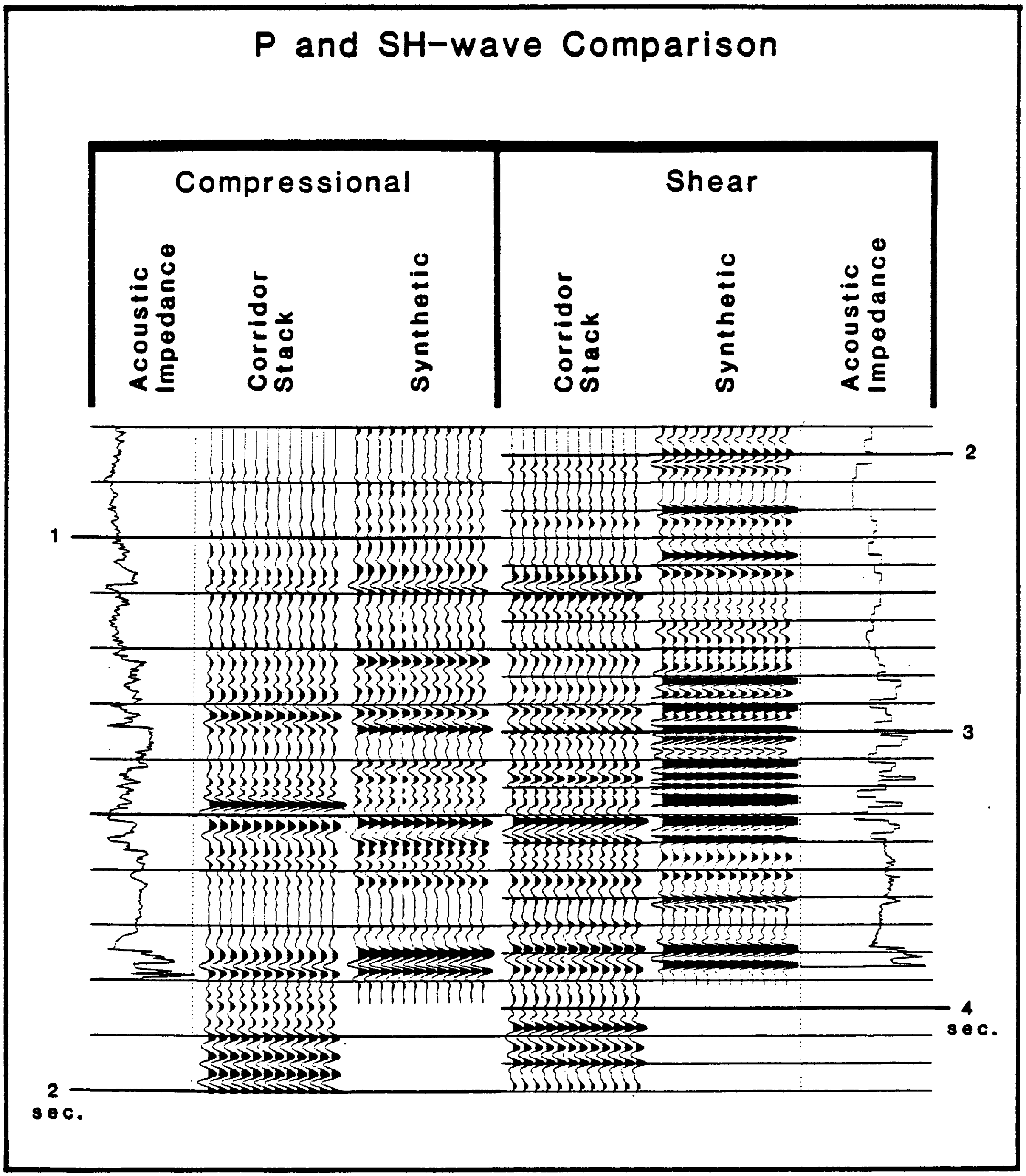

Figure 29. Correlation of P synthetic with VSP results from P- and SH-wave vibrators, 400 ft offset. Shear is plotted at half scale and tied to the Niobrara.

zero phase Ricker wavelet. The shear synthetic, presented for completeness only, was produced with a 17 Hz wavelet. The display is overdriven to prevent the large amplitudes between 3.1 and 3.4 sec from washing out the events below. Lacking waveform sonic data, shear synthetic amplitudes are wrong above 3.4 sec and only event occurence can be considered. Above 3.1 sec the VSP level spacing becomes too coarse for even this comparison.

Like the vertical P result, the offset P result of figure 30 displays good continuity and little noise. Velocities for moveout corrections were chosen to allow comparison with vertical results, affecting the alignment of some reflections.

To avoid deconvolving stretched traces, moveout corrections were applied after deconvolution. Excessive stretching of the offset trace above 1.3 sec distorts the comparison of vertical and offset compressional results in figure 31. Destructive interference from a transmitted P-SV event (fig 18) has weakened reflections between 1.9 and 2.0 sec in the offset corridor stack.

Converted Wave Extraction

Extraction of converted SV reflections proceeded without difficulty until the deconvolution stage of

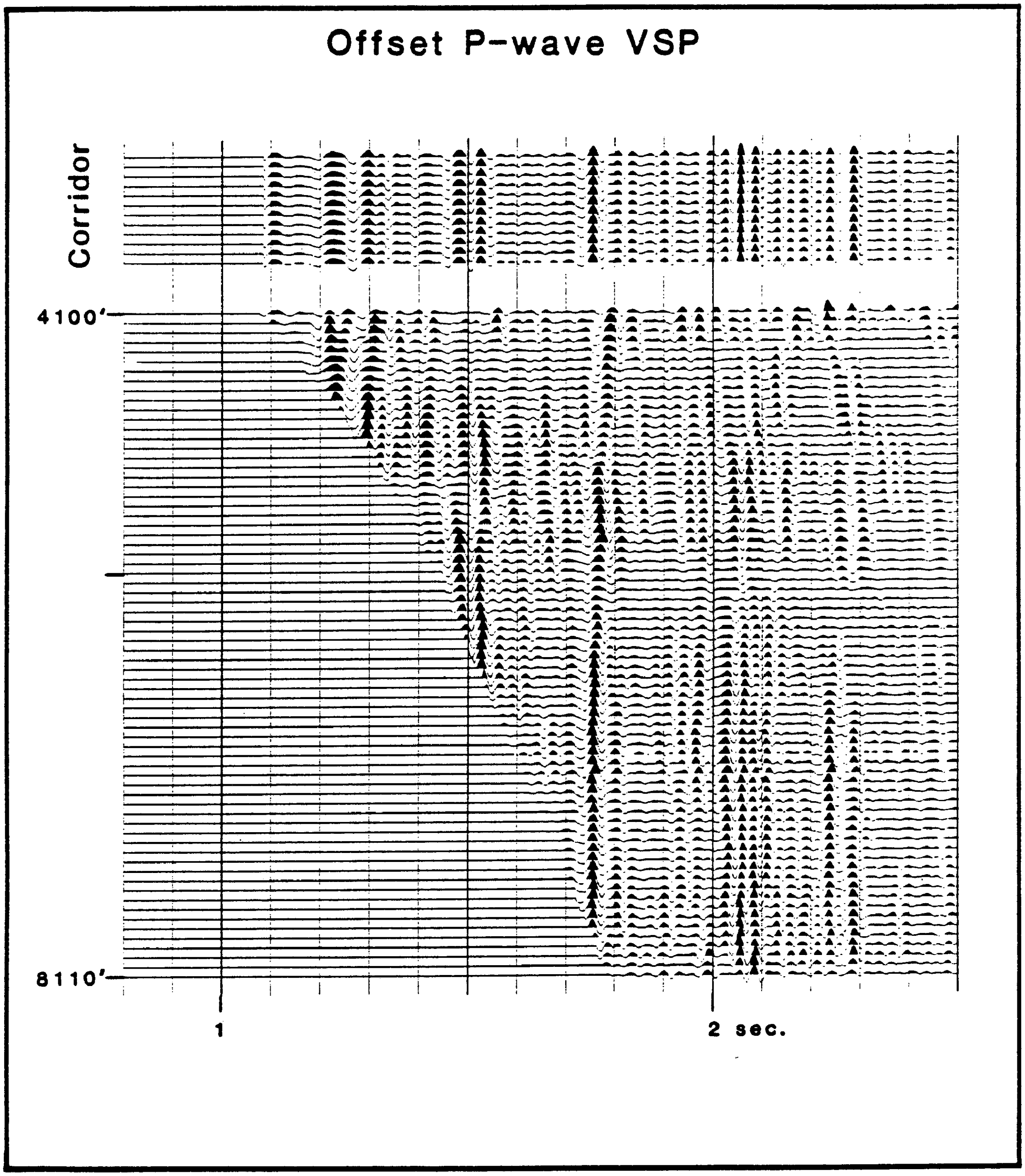

Figure 30. P results after deconvolution and moveout correction from P-wave vibrator, 4500 ft offset. NMO correction has stretched results above 1.3 sec.

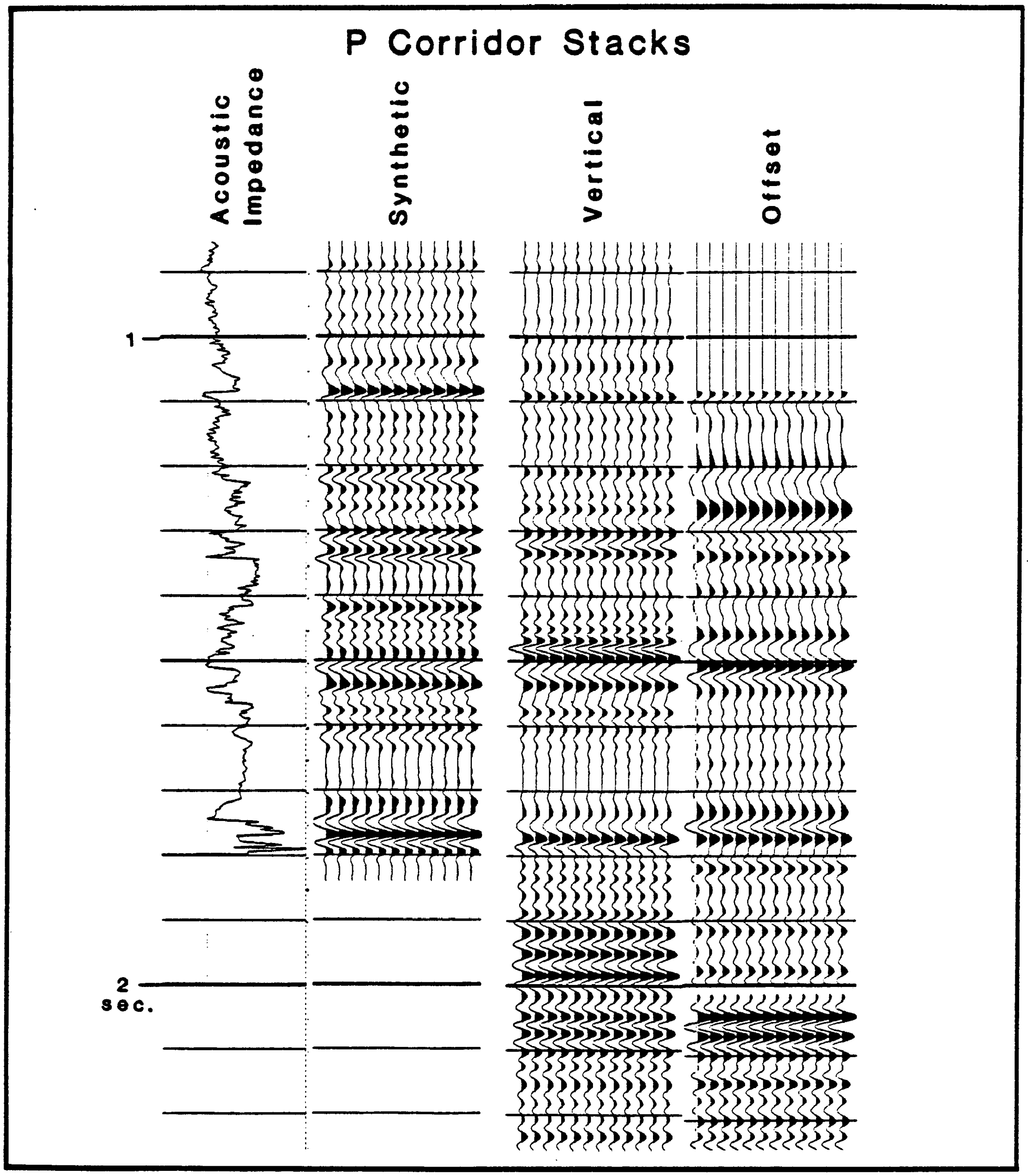

Figure 31. Correlation of P results from P-wave vibrators at 400 and 4500 ft offsets. Destructive interferance has weakened events at 1.9-2.0 sec in offset results.

processing. Choice of appropriate wavefields and interference from the direct shear arrival posed problems.

VSP deconvolution procedure uses a downgoing wave to design an operator for each level. This operator is then applied to the corresponding upgoing trace.

For converted P-SV reflections, deconvolution operators will be incorrect if they are designed from the downgoing shear wavefield. This downgoing wavefield consists of transmitted P-SV conversions and does not represent the multiples pattern of the reflected P-SV conversions.

Primary P-SV reflections are generated by the direct compressional arrival. The strongest reflected SV multiples should be generated by multiples of the direct compressional wave. Because of this, the downgoing compressional wavefield should be used to design the deconvolution operators for P-SV reflections.

These operators are applied to the upgoing shear wavefield of the transversely polarized record for the vertical survey. Upgoing shear events are enhanced by velocity filtering before deconvolution. The longitudinal record provides the upgoing wavefield for offset surveys.

Vertical and offset converted P-SV results are presented in figures 32 and 33. In the vertical case,

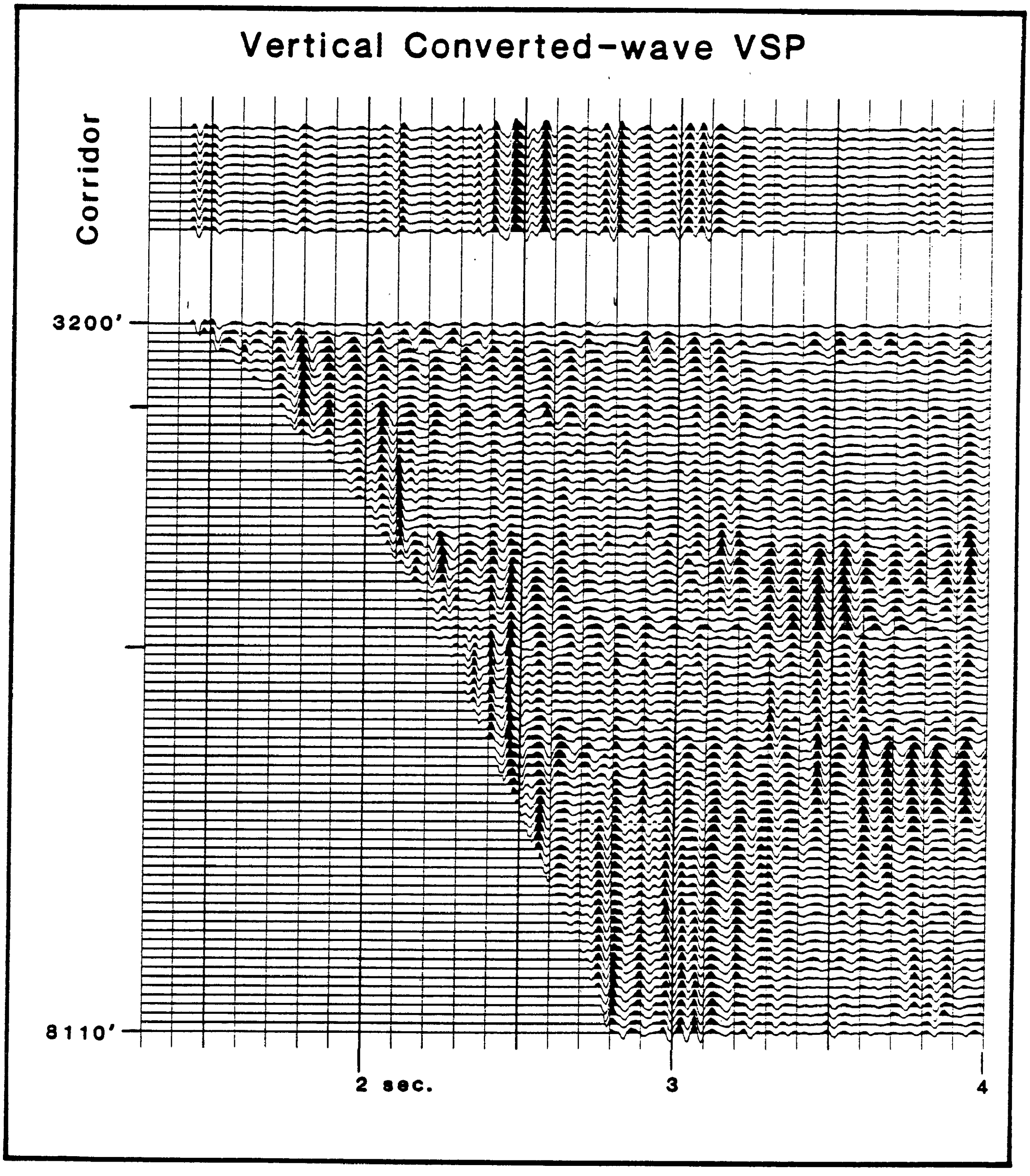

Figure 32. Converted P-SV results after deconvolution from P-wave vibrator, 400 ft offset. Ringing results are due to weak signal energy.

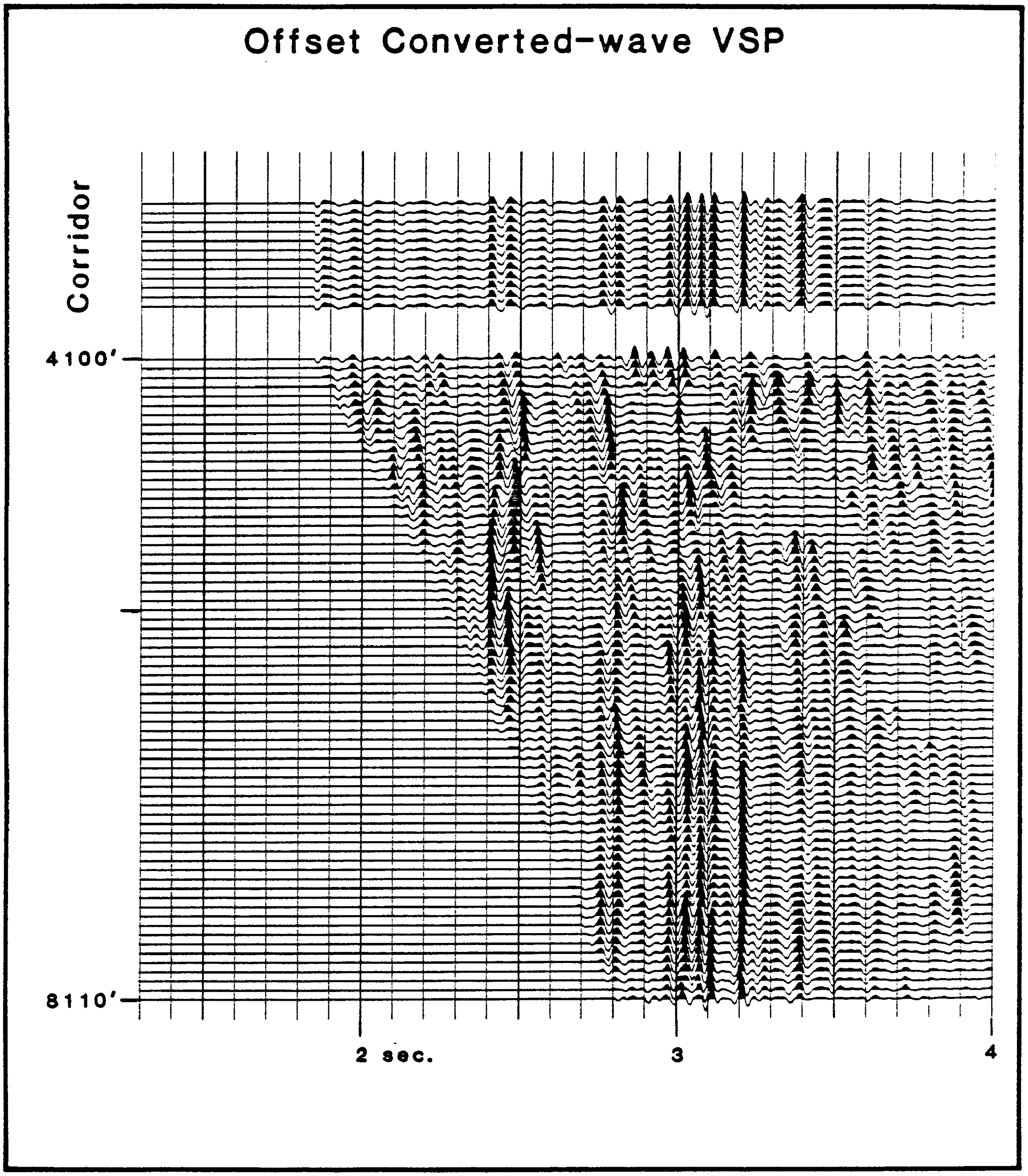

Figure 33. Converted P-SV results after deconvolution from P-wave vibrator, 4500 ft offset. Neither P nor S velocities are correct for moveout correction.

processing is being pushed to the limits. Modeling indicated reflected energy to be 2% of incident energy and the results are ringing.

Signal strength is much better in the offset survey, but moveout corrections proved difficult. To align events and place them properly in time, neither compressional nor shear velocities are correct. Moveout corrections have distorted the corridor stack above 2.4 sec. A balance must be struck between increasing offset to strengthen SV conversion and reducing offset to avoid distortion by moveout corrections.

Results after the direct shear arrival contain a mixture of P-SV and P-S-S reflections. Results near the first break are acceptable, but there were no strong downgoing multiples. In an area with strong multiples or bubble effect of offshore airguns, deconvolution results may prove unacceptable.

Transmitted Wave Extraction

Again, interference of the two reflected shear wavefields caused difficulties. Once the converted SV reflections cross the direct shear arrival, they can not be distinguished from the P-S-S reflections.

To reduce the effect of the converted reflections, the Hmin wavefield is used for processing. In theory, the P-SV conversions should not be present in this out-of-plane wavefield. In practice, they are very weak.

No useable results could be coaxed from the vertical data (fig 34) due to the poor signal to noise ratio of the horizontal minimun (energy) wavefield. Though noisy and weak at depth, the offset results (fig 35) do correlate with other shear corridor stacks (fig 36). Possibly the longer travel path through shallow layers caused more SV energy to be rotated in the offset geometry.

For the comparison of shear results, time scales have again been adjusted. The two way time ratio for converted to transmitted shear reflections is 3 to 4. (P two way time factor would be 2.) While events match reasonably well, character match across all four corridor stacks is poor. Separately, converted waves match each other well, as do the transmitted results. Stretch from moveout corrections severely distort both offset results.

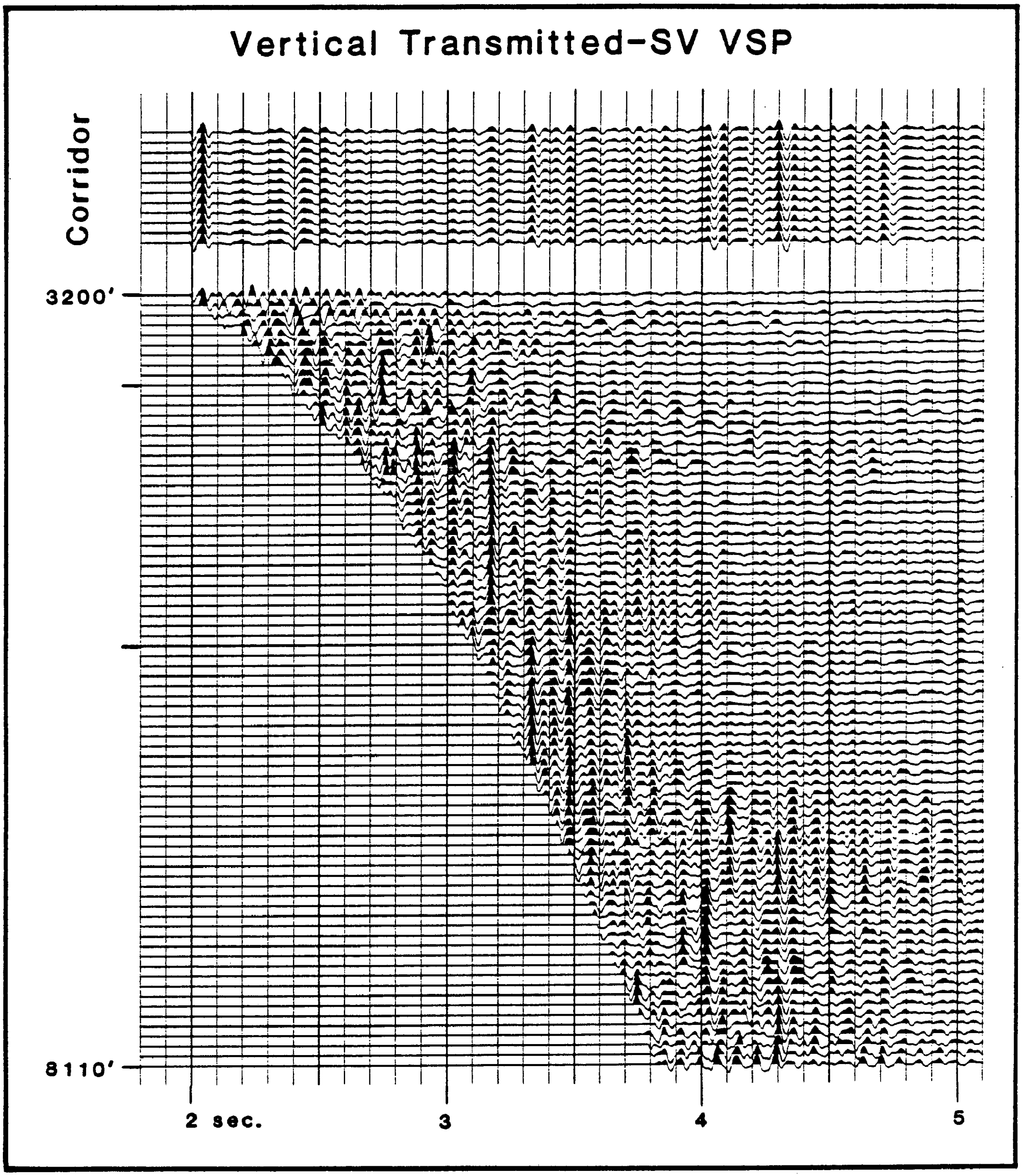

Figure 34. Converted P-S-S results after deconvolution from P-wave vibrator, 400 ft offset, contain only noise and do not correlate with other results.

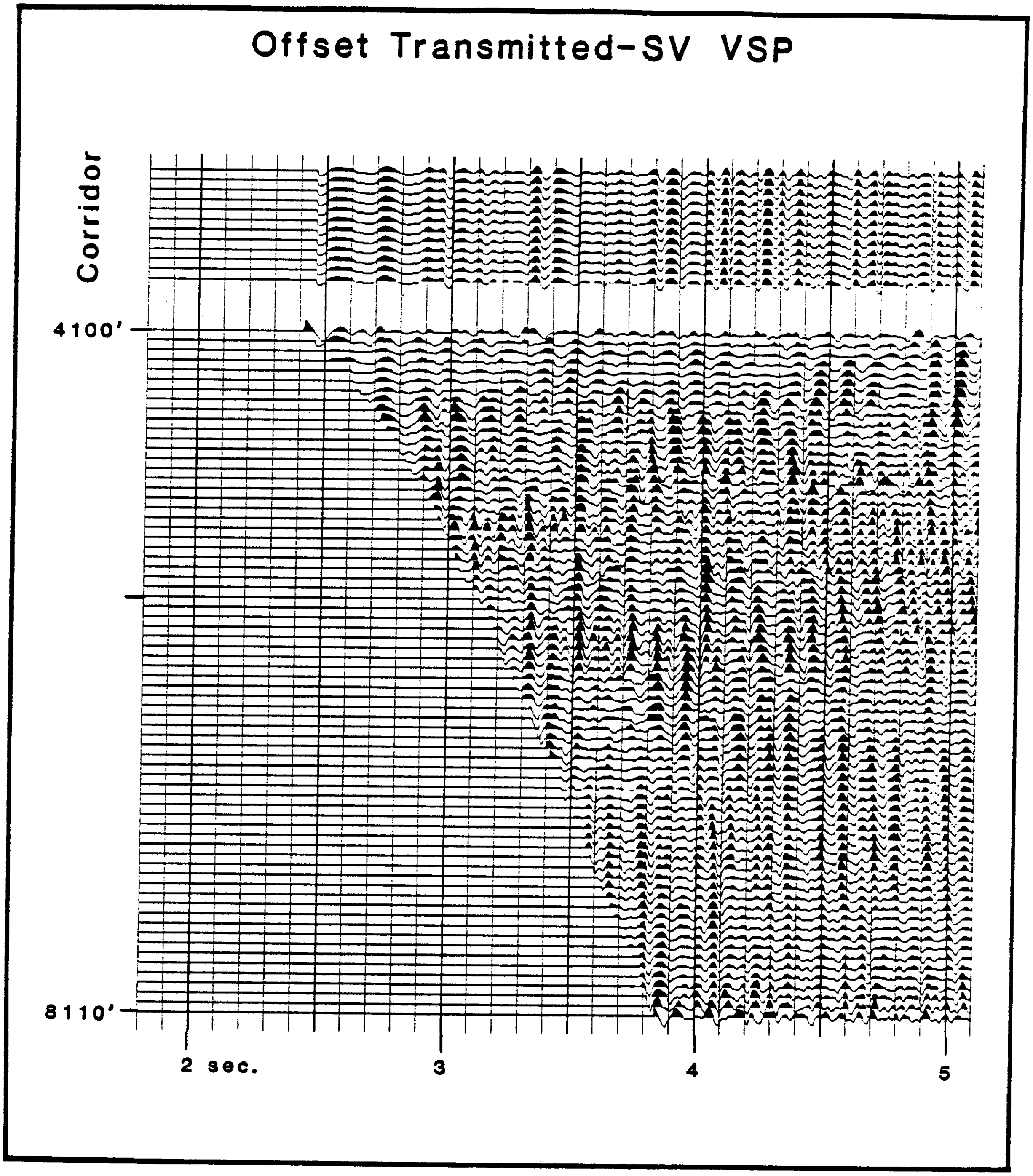

Figure 35. Converted P-S-S results after deconvolution from P-wave vibrator, 4500 ft offset. NMO stretch distorts results above 3.2 sec.

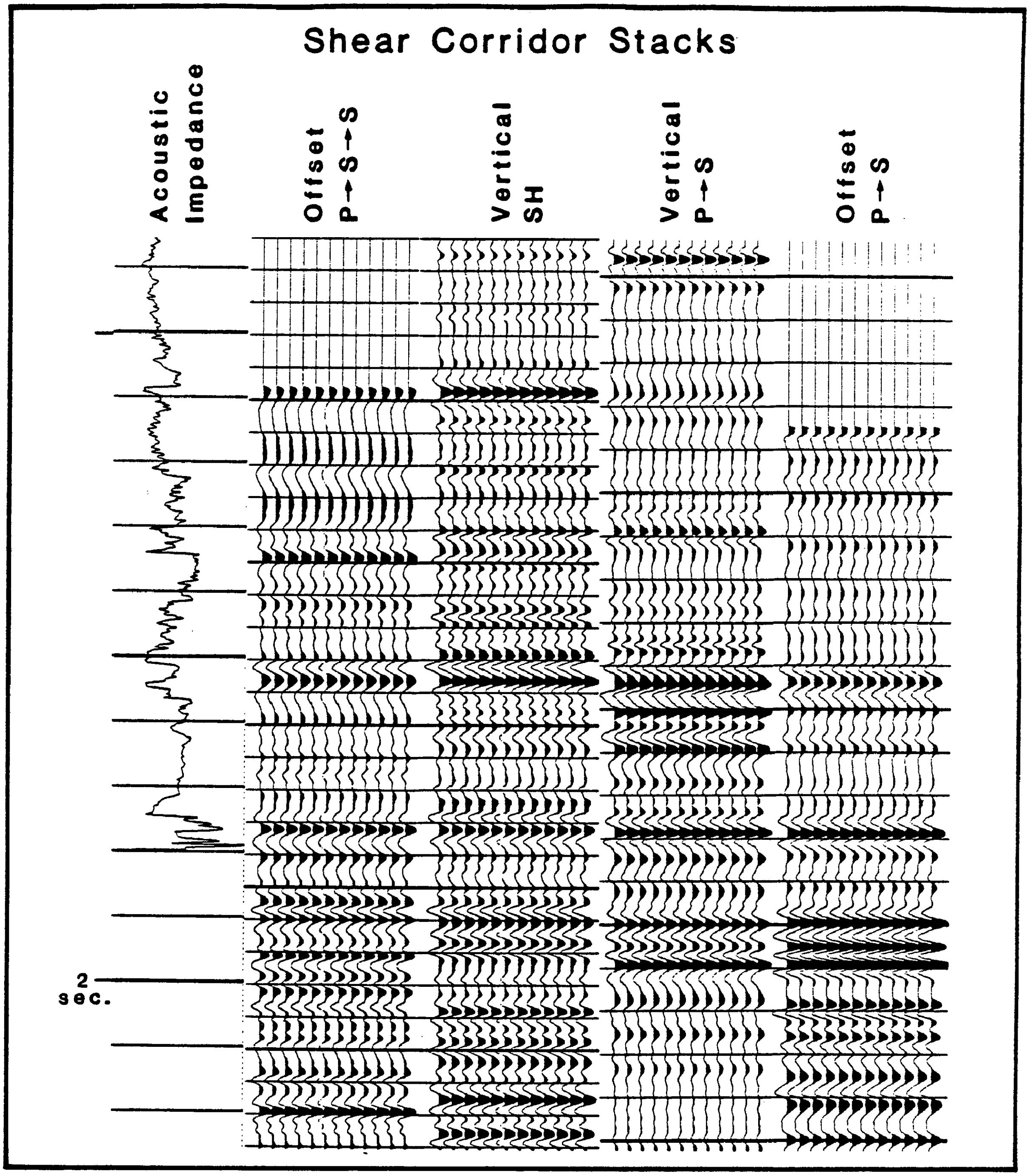

Figure 36. Correlation of extracted shear results from P-wave vibrators at 400 and 4500 ft offsets with results from SH-wave vibrator at 400 ft offset.

FUTURE WORK

Questions in the following areas appear to merit further investigation.

Processing

1) Can event and character matches be improved by better polarization or deconvolution procedures?

2) Can transmitted P-S conversions be used like reflection events to locate horizons?

3) Can a time-domain velocity filter be developed to account for the asymmetry of apparent velocities on offset data?

Interpretation

1) Can analysis of velocities, polarizations and amplitudes provide solid indications of fracturing or lithology and porosity identification?

2) Are observed variations in the presence of events and the character match of various modes consistent with theory?

3) Are the polarization and shear velocity anomalies discussed in Appendix C indications of anisotropy?

4) Are the shear events observed in this data set a common occurrance? If not, why is this set different and how could similar events be generated in other surveys?

CONCLUSIONS

Shear results can be extracted from compressional VSP surveys, using commercially available methods. Results of the same mode (P, SH or SV) generally show a good match of both events and character. Comparison of events between modes is fairly consistent, but character matches are often poor.

Amplitude differences may be due to different responses to the same horizon by different modes. Without information from a shear source, quantitative applications of converted results can not be made with confidence, until these differences can be explained.

Shear arrival times could be easily picked from polarized wavefields of compressional surveys in this experiment. This is necessary for processing and picks may not be as easy on every survey. Waveform sonic should be recorded and processed for shear velocities to verify VSP velocities and generate synthetics. The synthetic may help to confirm differences between compressional and shear results.

Converted and transmitted reflected wavefields interfere with each other in processing. Deconvolution is difficult. In an area with strong multiples or airgun bubble effect, deconvolution results may prove unacceptable. Lower frequency geophones should be used for shear measurement.

The various modes have been compared by choosing an appropriate time scale, tied at the Niobrara reflection. Correlations above and below this event depend on the assumption that the velocity ratio remains constant. Comparison after conversion from time to depth would be more accurate.

Polarization should be time variant for offset surveys, to be strictly correct. Despite this, polarization has performed well for compressional and shear energy. Polarization of converted P-S reflections is not correct. This is observed on wavefields and F-K plots. Raytrace modeling demonstrates these reflections are not normal to the direct arrival. A model based approach should be used for this wave mode.

Horizontal polarization angles can provide indications of fractures or anisotropy (Crampin). Results from vertical P surveys should be treated with caution as horizontal components are weak. Surveys should be recorded on the same pass to eliminate variations in tool orientation and coupling for comparison purposes.

Comparison of polarization angles from SH and P vibrators does not show rotation of the direct SH arrivals in the Niobrara. This does not preclude the presence of fractures. Logistics caused the shear source to be oriented so that SH waves were normal to the expected orientation of the vertical fracture plane, thus little if any rotation should be observed.

A qualitative inspection of the VSP reveals some indirect indications of fracturing. The amplitude of some direct shear arrivals appears to be reduced upon entering the Niobrara. Deeper reflections travel up through the Niobrara at a lower velocity than direct arrivals predict. This occurs in the bottom 6 traces of all VSP results and both P and S velocities are affected. There appears to be a difference between SH and SV velocities in the Niobrara. Quantitative investigations of amplitudes, velocities and polarization are required to verify these indications.

Offset increases converted shear energy but requires moveout corrections which distort results. These corrections are difficult in the P-SV case. This conflict should be resolved on an individual basis depending on the objectives of a particular survey.

Direct and reflected apparent velocities are not symmetric for long offset surveys. This violates a basic premise of time-domain velocity filters. Correction to zero moveout upsets wavelet similarity, affecting velocity filtering and deconvolution processes.

The Bolt Omnipulse source provides good, clean compressional and shear signals in one pass. Tilted shots can not be depended upon to provide sufficient compressional energy, vertical shots are required. The stacking technique should cancel tube waves on shear surveys. Arrival times agree with those observed from vibrator surveys.

The interval 3200-3600, in the Pierre shale, is anisotropic. SV velocities are higher than SH in this zone (Appendix C). This is theoretically expected in laminated solids for angles of incidence less than 50 degrees. Shear velocities, velocity ratios and polarization angles support this conclusion. Compressional velocities are only faintly disturbed in this zone. This interval does not differ from surrounding intervals on the gamma ray log or surface seismic.

When compared with examples published in the literature, the shear energy of this data set is unusually strong and coherent. There is no tube wave to obscure shear events. A surprising amount of shear energy is observed in the vertical compressional data. Good P-SV reflections are present from depths of 8000 ft with a source offset of only 400 ft, an incident angle of three degrees.

Is this a common occurance - or has a fortunate set of circumstances provided a rare example? Surveys traverse only two formations. Signals have passed through 5000 ft of Pierre shale, a formation frequently studied because of its unusual acoustic properties. The Niobrara below is known to be extensively fractured in this area.

SELECTED BIBLIOGRAPHY

Balch, A.H. and Lee, M.W., 1984, Vertical Seismic Profiling: Technique, Applications and case histories: Boston, IHRDC

Cheng, C.H., Keho, T., and Toksoz, M.N., 1982, Analysis of Tube Wave Data in Shear Wave VSP: presented at 52nd Annual International SEG Meeting, Dallas, Tx.

Corbin, R.J., Bell, D.W., and Danbom, S.H., 1983, Shear and Compressional-wave Surface and Downhole Tests in Southern Louisiana: presented at 53rd Annual International SEG Meeting, Las Vegas, Nev.

Crampin, S., 1985, Crack Porosity and Alignment from Shear Wave VSPs: intended for publication in SEG Special Publication "Shear-wave Exploration"

de Montmollin, V., 1983, Three-component Vertical Seismic Profile: Geometrical Processing and Wave Identification: presented at 53rd Annual International SEG Meeting, Las Vegas, Nev.

DiSiena, J.P., and Gasier, J.E., 1983, Three-component Vertical Seismic Profile:An Application of Gal'perin's Polarization Position Correlation Technique: presented at 53rd Annual International SEG Meeting, Las Vegas, Nev.

DiSiena, J.P., Gasier, J.E., and Corrigan, D., 1981, Three component Vertical Seismic Profile - Orientation of Horizontal Components for Shear Wave Analysis: presented at the 51st Annual International SEG Meeting, Los Angles, Ca.

Ensley, R.A., 1983, Direct Hydrocarbon Detection with P and SH-wave Seismic Data: presented at 53rd Annual International SEG Meeting, Las Vegas, Nev.

Gal'perin, E.I., 1974, Vertical Seismic Profiling: SEG special publication no. 12, J.E. White ed. (trans. from Russian by A.J. Hermont)

Gal'perin, E.I., 1984, The Polarization Method of Seismic Exploration: Dordrecht, Holland, D. Reidel Pub. (trans. from Russian by B. Kuznetsov and M. Samokhvalov)

Gasier, J.E., Ward, R.W., and DiSiena, J.P., 1982, Three component Vertical Seismic Profile: Polarization Measurements of P-wave Particle Motion for Velocity Analysis: presented at 52nd Annual International SEG Meeting, Dallas, Tx.

Hardage, B.A., 1983, Vertical Seismic Profiling Part A: Principles: London, Geophysical Press

Oristaglio, M.L., Devaney, J.A., and Track, A., 1985, Separation of P-waves and S-waves in Borehole Seismic

Data: presented at 55th Annual International SEG Meeting, Washington, D.C.

Panziera, J.P., and Arens, G., 1985, Three-component Vertical Seismic Profiles: Polarized Wave Separation: presented at 55th Annual International SEG Meeting, Washington, D.C.

Postma, G.W., 1955, Wave Propagation in a Stratified Medium: Geophysics, Vol. 20, p.780-806.

Robertson, J.D., and Pritchett, W.C., 1983, Bright Spot Validation Using Comparative P-Wave and S-wave Seismic Sections: presented at 53rd Annual International SEG Meeting, Las Vegas, Nev.

Robertson, J.D., 1983, Carbonate Porosity from S/P Traveltime Ratios: presented at 53rd Annual International SEG Meeting, Las Vegas, Nev.

Toksoz, M.N. and Stewart, R.R. ed., 1984, Vertical Seismic Profiling Part B: Advanced Concepts: London, Geophysical Press

White, J.E., 1983, Underground Sound - Application of Seismic Waves: New York, Elsevier.

APPENDIX A

OMNIPULSE

As a source comparison test, two 15 level surveys were recorded over the interval 5950 to 7000 ft, using the Bolt Omnipulse source. Two sources were used at a 400 ft offset while only one was available for the survey at 1500 ft offset.

The Omnipulse is a truck mounted 400 cubic inch airgun with teeth fixed to the base of the pad to facilitate transmission of shear energy into the ground. The airgun can be fired in either a vertical orientation, as a compressional source, or with the chamber tilted 45 degrees left or right, generating a mixture of P and S waves.

Adding shots with left and right tilts, stacks P waves while canceling S waves. Subtracting left tilt shots from shots tilted right, stacks S waves and cancels P waves. Conceivably, this technique would also cancel tube waves on shear records.

Stacks of figure 37 demonstrate the effectiveness of the principle. The strong direct arrivals and clean records on the Z axis of the P stack contrast sharply with

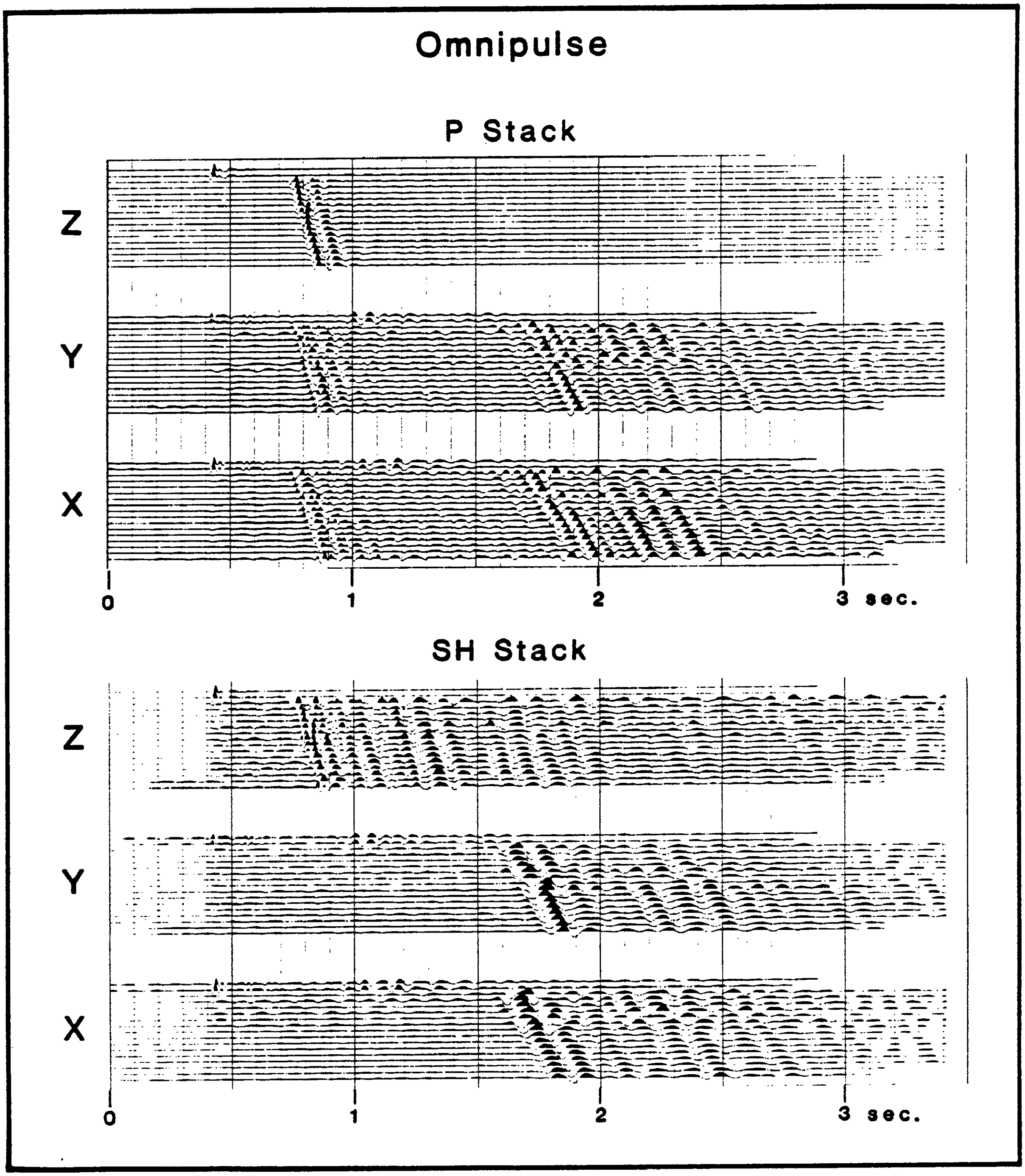

Figure 37. P and S stacks from Omnipulse source, 400 ft offset, demonstrate the effectiveness of the stacking principle. Top two traces are shallow test shots.

the shear stack Z axis where direct arrivals are no larger than later noise.

The horizontal axes of the shear stack show strong, coherent shear energy with little noise before the shear arrival and no evidence of a compressional arrival. Shear stacking has effectively canceled the compressional activity observed on the horizontal axes of the P stack. The shear events on the P stack are of higher frequency than that of the shear stack. The same relationship occurred on the vibroseis data. Arrival times of the Omnipulse agreed with those from the vibrator sources +/- 2 ms.

Corridor stacks of these surveys after waveshaping deconvolution are compared with vibrator corridor stacks in figure 38. The Omnipulse survey only covered 15 levels, thus there are no results above 1.42 sec. Events after 1.6 sec are below the deepest shot. Airgun shear events correlate well and appear to contain higher frequencies.

Only two shots at each level were taken with the gun in the vertical orientation. It was assumed the P energy from tilted shots (eight each side) would be sufficient. The washed out appearance of the Omnipulse compressional corridor stack suggests more P energy is needed and more vertical shots should be taken.

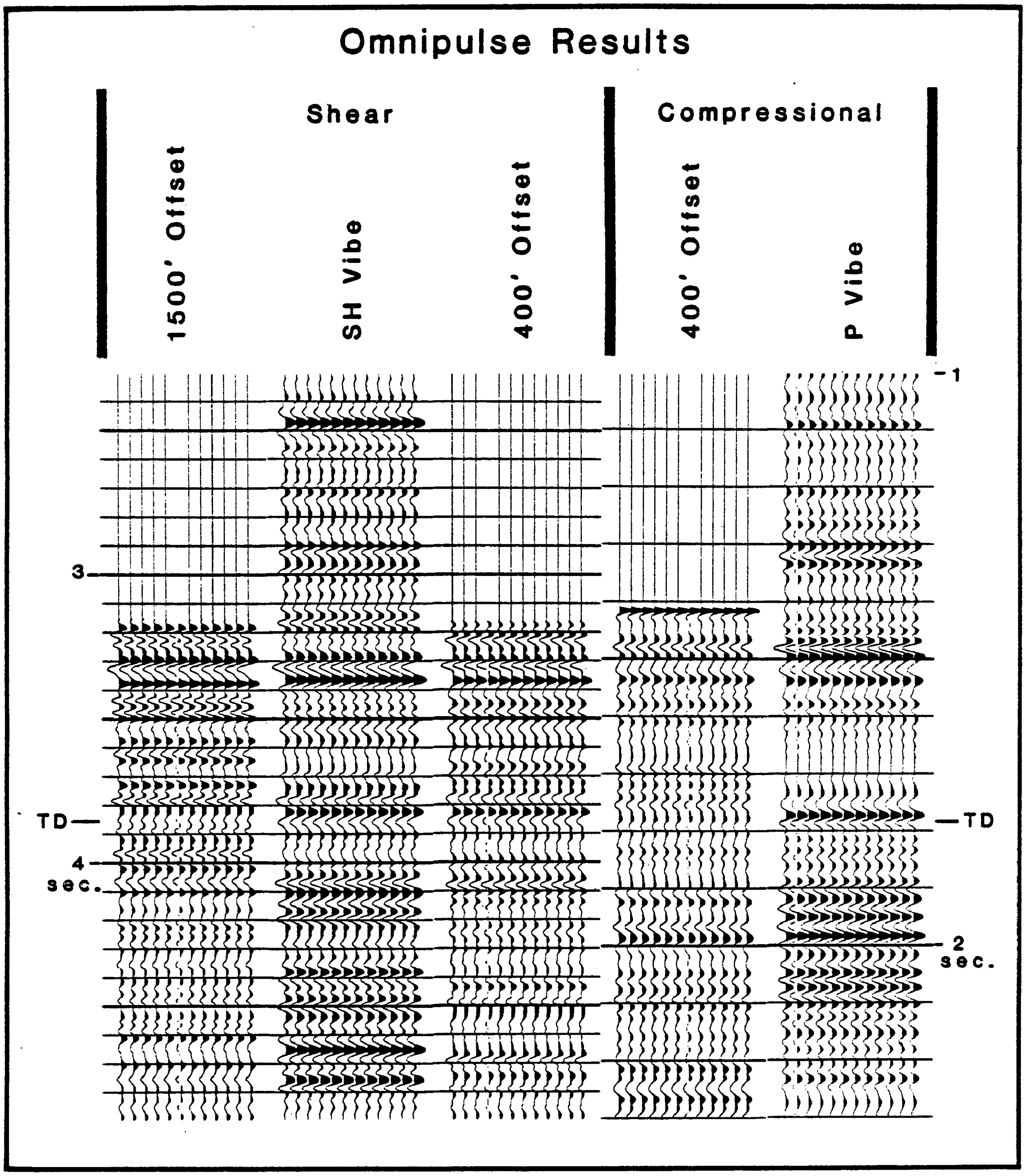

Figure 38. Correlation of corridor stacks from Omnipulse with P- and SH-wave vibrators, 400 ft offset. Airgun survey covered the interval 1.42-1.6 sec only.

APPENDIX B

HORIZONTAL POLARIZATION ANGLES

The vertical P, vertical SH and offset P surveys were acquired during one pass in the well. Signals were recorded from each source before moving the tool to the next level, eliminating variations in tool orientation and coupling when comparing these surveys.

Horizontal polarization angles indicate tool orientation and should agree on all three surveys, allowing for source position geometry. Variations in apparent shear orientation are theoretically due to anisotropy or fracturing.

The sources were positioned along an east-west line 180 ft south of the well. The 400 and 4500 ft offset figures are direct well-to-source distances. Thus, the compressional survey angles should differ by a constant 27 degrees. The shear vibrator was oriented to provide SH waves and should differ from the vertical compressional by 90 degrees or 63 degrees from the offset.

Since offset P angles should be the least ambiguous, they are taken as the reference for the plots of figure 39. Level zero is the deepest level. To compare

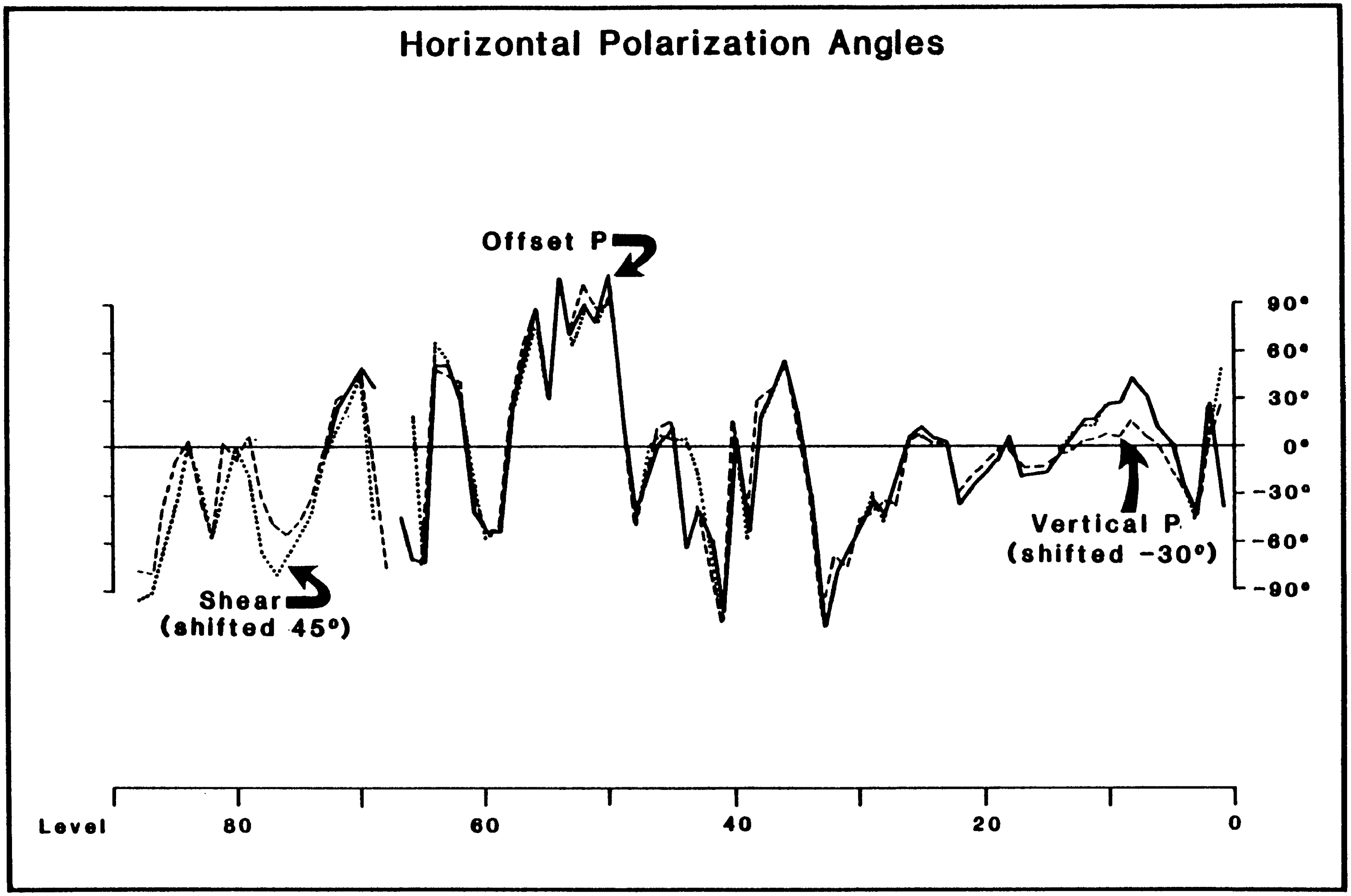

Figure 39. Horizontal polarization angles from vertical and offset vibrators indicate tool orientation. Vertical curves shifted a constant amount to overlay.

with the offset P reference, curves from both vertical sources are shifted a constant amount at each level. To match the offset curve, angles from the vertical P source must be shifted -30 degrees, which compares well with the -27 degrees calculated above.

Shear angles must be shifted 45 degrees to match the offset P curve. This is 15 degrees different from the value expected from calculations. Since shear angles agree over the entire survey, it seems the shear vibrator was actually rotated 15 degrees east of the desired orientation.

The horizontal component of the vertical P survey is very weak, especially at depth, thus confidence in these angles is low. Given this, the correlation is surprisingly good and divergence at deeper levels can be explained.

The shear angle diverges from that of the compressional at levels 77-79. This interval (3500-3700 ft) corresponds to the section of high V_p/V_s ratio and is believed to be anisotropic. (see Appendix C).

Comparison of polarization angles from SH and P vibrators does not show rotation of the direct SH arrivals in the Niobrara. This does not preclude the presence of fractures. Logistics caused the shear source to be oriented so that SH waves were normal to the expected orientation of the vertical fracture plane, thus little if any rotation should be observed.

APPENDIX C

VELOCITY OBSERVATIONS

Asymmetry of apparent velocities in offset data.

Raypaths suggest that downgoing velocities are not symmetric with upgoing velocities for offset configurations. The disparity increases for shallower levels. This violates a basic assumption of most (all?) time-domain velocity filters.

The F-K plots support this observation of velocity asymmetry noted on ray trace models. All vertical data, both up and downgoing, display P velocities of 11450 ft/sec and S velocities of 5790 ft/sec. Offset plots contain a range of velocities for each wave mode and all velocities are higher than those observed for the vertical data. Additionally, downgoing velocities are higher than upgoing. Downgoing shear velocities range from 6560 ft/sec to 8100 ft/sec while the corresponding reflected waves travel between 5790 ft/sec and 6560 ft/sec. For compressional waves, the respective ranges are 13450 - 15000 ft/sec and 12100 - 13450 ft/sec.

Anisotropy

Differences of shear wave velocities are observed near the top of several records. This effect may be due to formation characteristics and could severely affect surface shear results.

Hmax and Hmin are well aligned for the shear source (fig 40) but records from the compressional sources (fig 41), especially the Hmax component, deviate from alignment near the top of the data. Data from both vertical sources has been aligned to arrival times of the SH vibrator.

The ringing arrivals along with this disparity can not be a tube wave because ringy events clearly appear in vertical P Hmax traces above the top of fluid, known to be at 2800 ft in this well. The moveout of traces requires a velocity higher than shear which averages 5790 ft/sec from F-K plots, and tube wave velocity is calculated to be 4350 ft/sec. F-K plots show no appreciable energy at tube-wave velocity. Further, there is no reflection from the bottom of the well and particle motion is predominately horizontal, not vertical (figs 9, 10, 11). While a tube wave must be present, it is not observed because the anchoring force of this tool is 440 lbs., and tool weight is only 175 lbs.

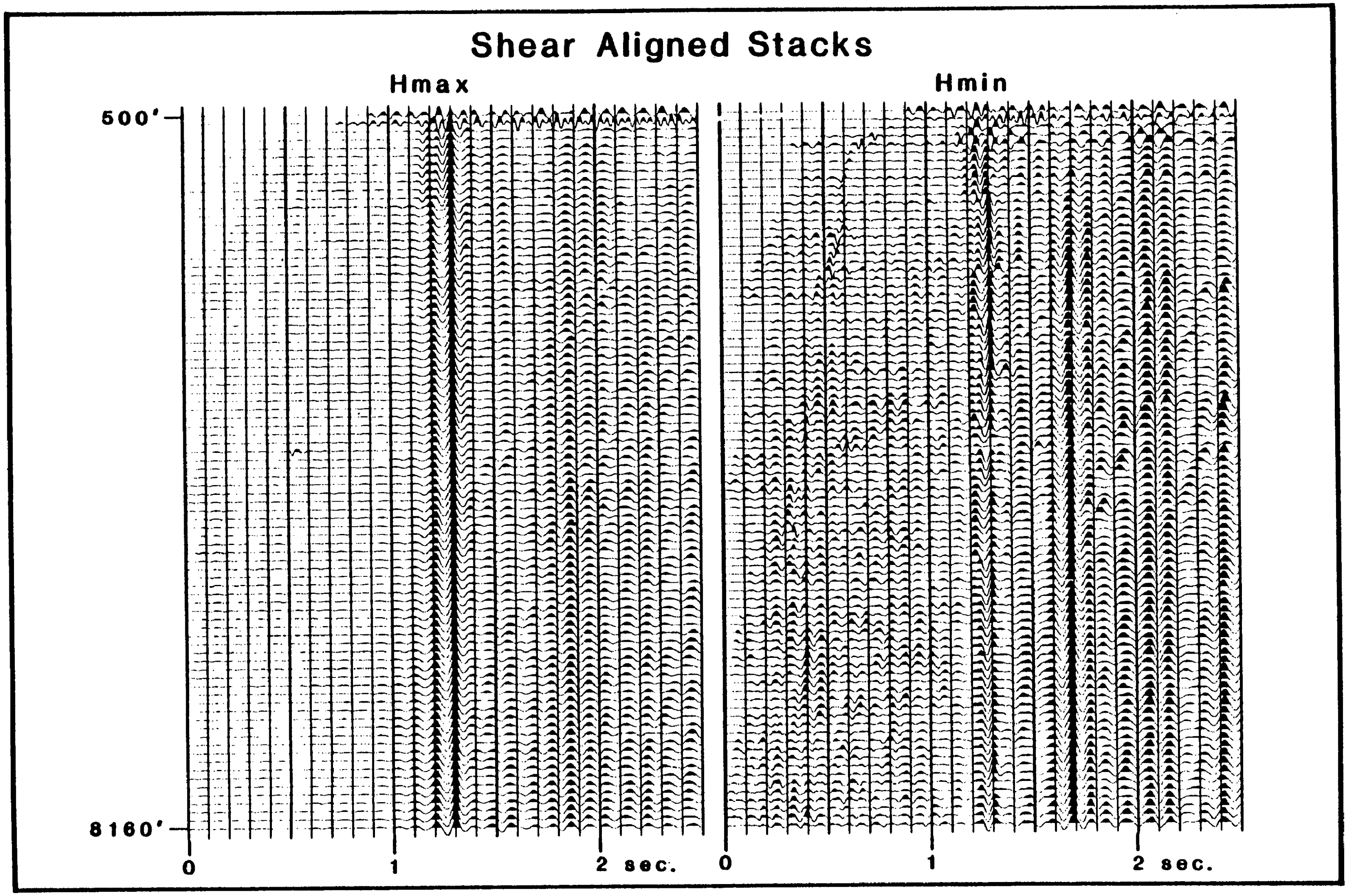

Figure 40. Stacks of polarized horizontal axes from 400 ft offset, SH-wave vibrator. Events are aligned to direct arrival times of SH-wave survey.

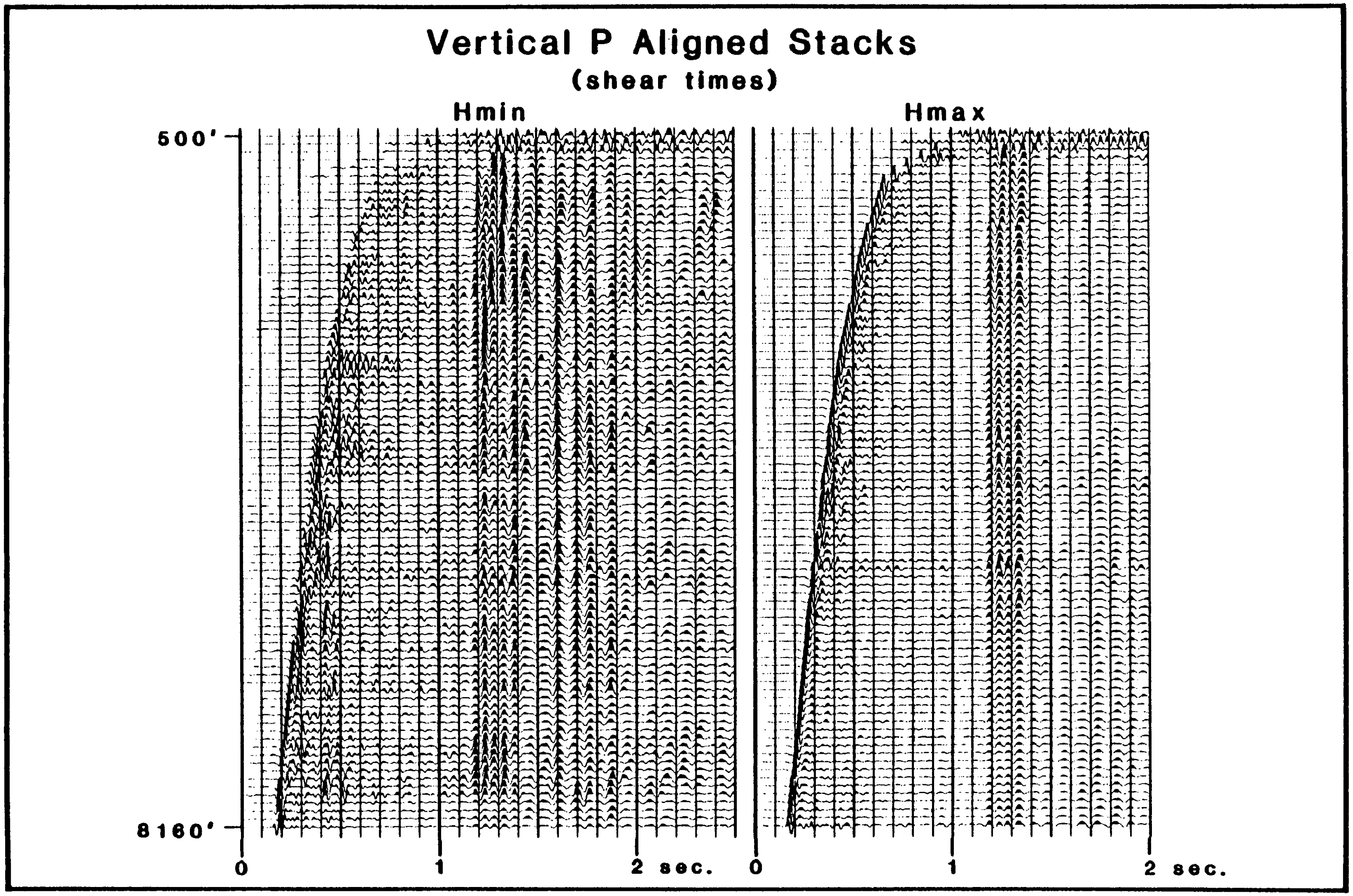

Figure 41. Stacks of polarized horizontal axes from P-wave vibrator, 400 ft offset. Events are aligned to direct arrival times of SH-wave survey.

On vertical records, the shift appears abruptly above the trace at 3600 ft. A change in wavelet can be seen at this point on shear source records. Coincidentally, the V_p/V_s ratio abruptly changes and the horizontal polarization angles from P and SH sources diverge at this depth.

All this could be due to poor arrival time picks. Changing break picks to align the vertical P Hmax wavefield only shifts the velocity ratio and misaligns the SH wavefields. Changing picks to remove the ratio anomaly (3400-3600 ft) introduces unacceptable alignment of all horizontal wavefields.

The alignment disparity is more pronounced on the offset data (fig 42). The offset data is aligned to shear arrival times picked from the offset Hmin component. While the apparent velocity of the Hmax wavefield differs from that of the Hmin throughout the data set, major divergence begins at approximately 5100 ft. Notice, from the direct P raypaths in figure 19, that the length of direct rays through the 3150-3600 interval begins to noticeably increase for arrivals above 5400 ft.

The offset Hmin wavefield does not behave in this manner. Observe in figure 43 that this record is the only compressional wavefield whose wavelet and multiple patterns

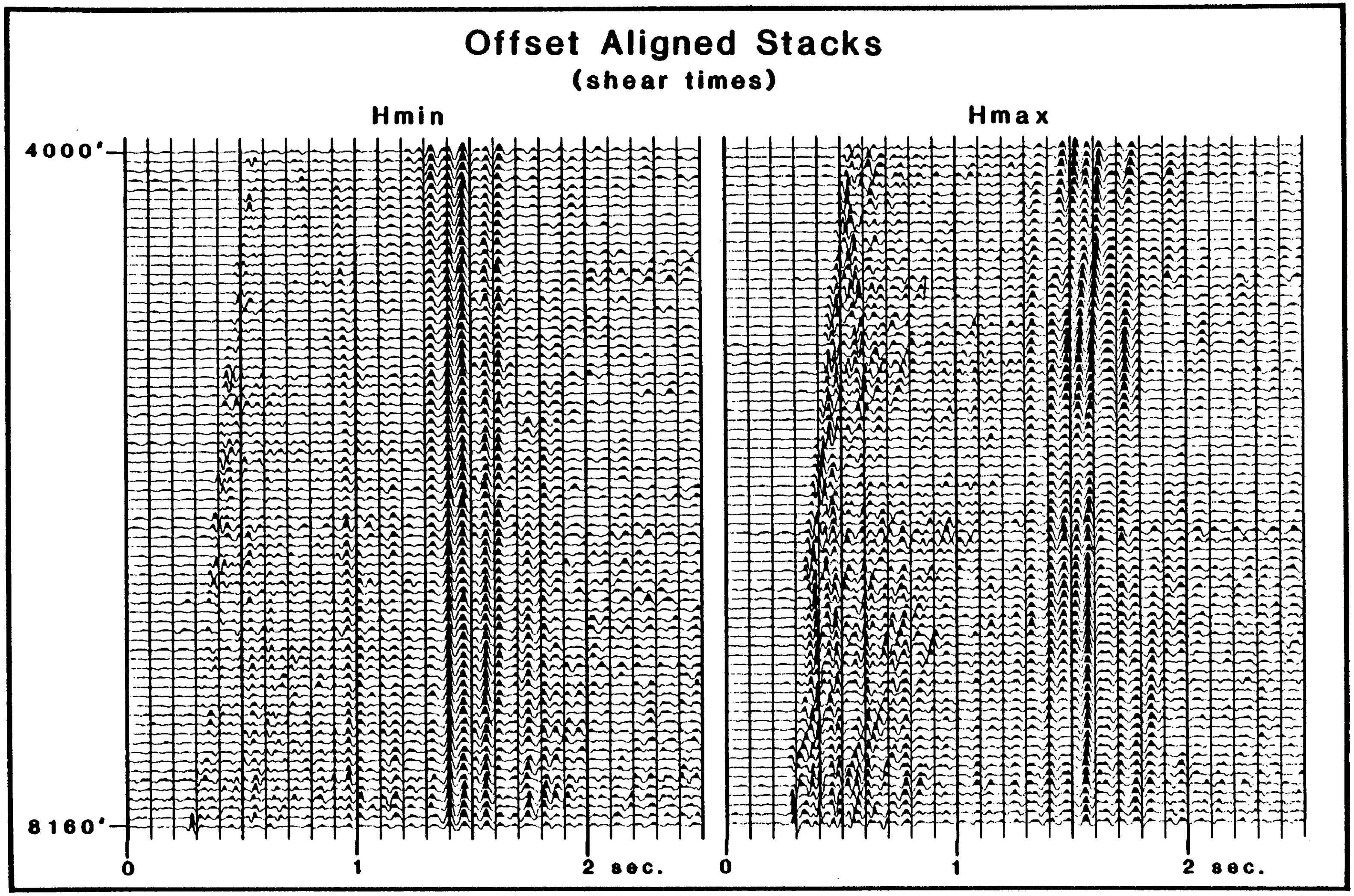

Figure 42. Stacks of polarized horizontal axes from P-wave vibrator, 4500 ft offset. Events are aligned to arrival times picked from Hmin.

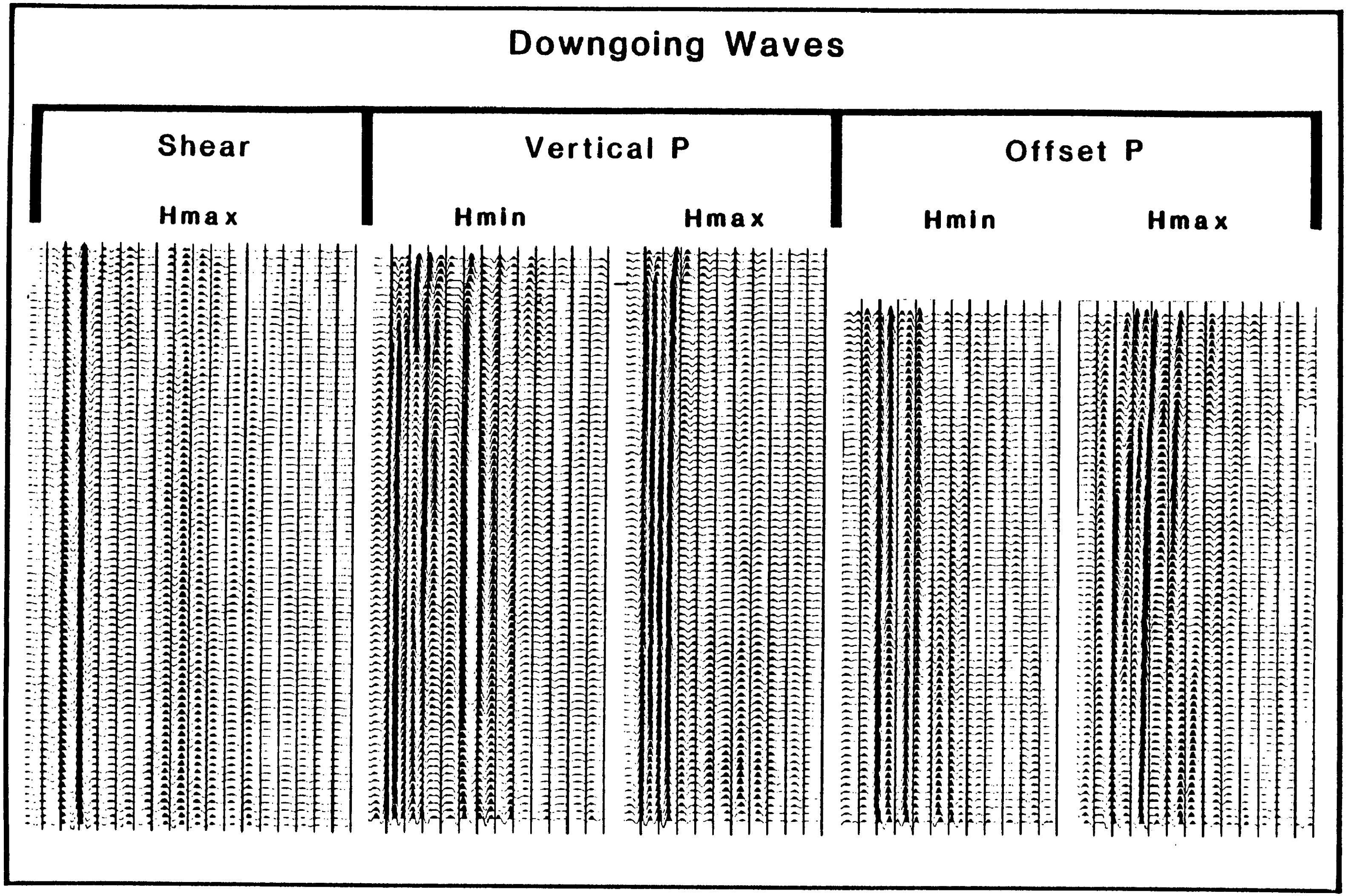

Figure 43. Downgoing shear waves after velocity filtering from polarized horizontal axes of vertical and offset vibrator sources.

resemble that from the SH source.

These phenomena are consistent with theoretical expectations of velocities in laminated solids (White 1983 pp53-55). SV velocity could be higher than SH velocity for angles of incidence less than 50 degrees.

This possible explanation can not be confirmed with the information currently available. The interval in question does not differ from its surroundings on either the compressional surface seismic or the gamma ray log in this well. No detailed geologic information about this interval of the Pierre shale is available.

APPENDIX D

POLARIZATION

The downhole tool records X, Y, and Z axes without orientation information. The tool rotates and randomly orients the horizontal X and Y axes from level to level. To analyse and correlate signals from these axes, the components must be correctly oriented to some fixed reference axes.

Polarization is performed in two stages, as illustrated in figure 7. Hodograms, polarization angle and correlation coefficients are used to monitor the quality of the process.

Assuming linear polarization of the direct arrival from a compressional source, particle velocity will be along rays pointing towards the source. The maximum particle velocity observed in the horizontal components will then always point towards the source, establishing a fixed reference axis consistent from level to level, irrespective of tool rotation.

Hodograms (Fig 8) display the velocity trajectory by plotting X(t) versus Y(t) in a small time window surrounding the first arrival. Because records are contaminated by noise, the curve should be an ellipse rather than a straight line. The major axis defines the main direction of energy arrival in the horizontal plane.

The direction of the major axis is determined by a line passing through the origin and fit to the cloud of points on the hodogram. Once this axis is determined, a coordinate transformation from (X,Y) to (Hmax,Hmin) is computed by:

$$Hmax = X\cos(A) + Y\sin(A)$$

$$Hmin = -X\sin(A) + Y\cos(A)$$

where A is the angle between the major axis and the X geophone. The Hmax axis is in the direction of maximum particle velocity with the Hmin axis perpendicular to this (not a true minimum if the ellipse is skew).

The Hmax axis represents the in-plane motion of P and SV waves, while Hmin should enhance the uncoupled SH wavefield. If we had a pure P-SV source, a true visco-elastic medium and perfect horizontal layering, we should observe only noise in the Hmin axis.

Components of the in-plane P-SV wavefield can be further enhanced by polarizing the Z and Hmax axes into longitudinal and transverse axes. These final axes represent particle velocity in line with and normal to the ray of the direct P arrival respectively.

As illustrated in figure 7, the longitudinal wavefield tends to enhance direct P and reflected SV energy for offset sources. The transverse wavefield then enhances reflected P and direct SV energy. For small offset configurations, the longitudinal axis represents the P wavefield while the transverse axis contains the total SV energy.

By velocity filtering, individual wave modes of interest can be further enhanced while supressing undesired modes. For example, if SV waves from an offset source are desired, velocity filter the transverse wavefield for the downgoing SV and the longitudinal wavefield for the upgoing SV. Processing then proceeds as for the classical single component VSP.

The preceeding approach is a signal based method, using the recorded signal without recourse to external knowledge. The degree of success of this method is dependent on offset and velocity contrasts. Reflected waves are exactly normal to direct arrivals only over a few levels in any survey. Refractions can radically alter the arrival angle of direct waves, distorting polarization results of the reflected energy. (see MODELING section) This procedure provides a good direct P signal, but reflected energy is not strictly correct.

A model based approach could avoid some of the problems by "forcing" polarization. This would overcome some offset and refraction effects but success is dependent on an accurate model. Being processor dependent, this violates the thesis objective of a "commercial" solution.

Polarization should be time variant to be strictly correct for offset surveys. For a given level, the incident angle of reflection events arriving later in the trace, from deeper horizons, will be different from events generated by horizons close to the level (fig 8).

For shear energy, an early assumption is violated when polarization is non-linear (fractures or anisotropy). As models can not account for such effects, the signal based method should be used. The hodogram window should be placed over a strong downgoing shear event, if one is present.

All these procedures assume input data from a properly designed tool having identical amplitude and phase response for all geophones. For reasons stated above, geophone response versus incident angle complicates amplitude studies of offset VSP data.

APPENDIX E

VSP DEPTH and ARRIVAL TIMES

	Depth (ft)	Arrival Times (ms) P	SH	Offset		Depth (ft)	Arrival Times (ms) P	SH	Offset
1	8160	894	1926	1003	46	5900	693	1530	849
2	8110	889	1920	998	47	5825	688	1519	843
3	8060	885	1911	997	48	5775	684	1512	840
4	8010	883	1906	993	49	5750	679	1505	840
5	7960	879	1899	990	50	5700	675	1501	836
6	7940	877	1896	987	51	5625	671	1486	833
7	7900	873	1886	985	52	5550	664	1474	829
8	7850	868	1875	980	53	5475	658	1462	825
9	7800	863	1867	977	54	5400	650	1446	818
10	7750	858	1859	973	55	5325	644	1434	814
11	7700	854	1850	969	56	5250	638	1423	811
12	7650	849	1839	967	57	5175	631	1412	806
13	7600	845	1830	962	58	5100	624	1398	803
14	7550	841	1822	959	59	5025	617	1385	799
15	7500	837	1814	956	60	4950	610	1371	795
16	7450	833	1806	953	61	4875	603	1356	790
17	7400	829	1798	948	62	4800	597	1341	787
18	7350	823	1789	945	63	4725	590	1324	783
19	7300	820	1781	941	64	4650	581	1309	777
20	7250	817	1773	939	65	4575	574	1294	773
21	7200	811	1765	935	66	4500		1279	769
22	7100	807	1756	933	67	4425			765
23	7100	803	1748	927	68	4424			765
24	7050	798	1740	926	69	4400	557		
25	7000	794	1732	923	70	4325	551	1247	760
26	6950	790	1723	919	71	4250	544	1233	756
27	6900	786	1715	917	72	4175	537	1220	754
28	6850	780	1705	911	73	4100	529	1205	749
29	6800	777	1697	908	74	4000	520	1187	744
30	6750	772	1687	905	75	3900	511	1165	
31	6700	764	1679	900	76	3800	500	1145	
32	6650	762	1672	896	77	3700	489	1126	
33	6600	757	1663	893	78	3600	480	1106	
34	6550	753	1645	890	79	3500	470	1071	
35	6500	750	1639	886	80	3400	459	1050	
36	6450	743	1632	883	81	3300	449	1024	
37	6400	737	1622	878	82	3200	438	1003	
38	6350	733	1609	873	83	3100	428	981	
39	6300	729	1601	873	84	3000	419	961	
40	6250	725	1591	869	85	2500	369	856	
41	6200	721	1585	867	86	2000	314	737	
42	6150	716	1576	865	87	1500	257	607	
43	6100	711	1568	861	88	1100	208		
44	6050	706	1560	859	89	1000	195	450	
45	5975	699	1544	853	90	500	135	289	